Skarns and Skarn Deposits

Lawrence D. Meinert
Department of Geology
Washington State University
Pullman, Washington 99164-2812 USA

SUMMARY

Skarn deposits occur throughout the world and have been mined for a variety of elements. This paper describes the basic stages of skarn formation and the main causes of variation from the general evolutionary model. Seven major classes of skarn deposits (Fe, W, Au, Cu, Zn, Mo and Sn) are briefly described, and relevant geological and geochemical features of important examples are summarized in a comprehensive table. The important geochemical and geophysical parameters of skarn deposits are discussed, followed by a summary of important petrologic and tectonic constraints on skarn formation. Finally, exploration models are presented for several major skarn types, with a plea for field mapping as a fundamental basis for future studies.

INTRODUCTION

Skarn deposits have been mined for a variety of elements, including Fe, W, Cu, Pb, Zn, Mo, Ag, Au, U, REE, F, B and Sn. Skarns occur on all continents and in rocks of almost all ages. Although the majority are found in lithologies containing at least some limestone, they can form in almost any rock type, including shale, sandstone, granite, basalt and komatiite. Skarns can form during regional or contact metamorphism and from a variety of metasomatic processes involving fluids of magmatic, metamorphic, meteoric and/or marine origin. They are found adjacent to plutons, along faults and major shear zones, in shallow geothermal systems, on the bottom of the sea floor, and at lower crustal depths in deeply buried metamorphic terranes. What links these diverse environments, and what defines a rock as skarn, is the mineralogy, which includes a wide variety of calc-silicate and associated minerals, but is usually dominated by garnet and pyroxene. Thus, the presence of skarn does not necessarily indi-

cate a particular geologic setting or a particular protolith composition. Rather, its development indicates that the combination of temperature, pressure, fluid and host rock composition was within the stability range of the identified skarn minerals.

Just as mineralogy is the key to recognizing and defining skarns, it is also critical in understanding their origin and in distinguishing economically important deposits from interesting but uneconomic mineral localities. Skarn mineralogy is mappable in the field and serves as the broader "alteration envelope" around a potential ore body. Be-

cause most skarn deposits are zoned, recognition of distal alteration features can be critically important in early exploration stages. Details of skarn mineralogy and zonation can be used to construct deposit-specific exploration models, as well as more general models useful in developing grass-roots exploration programs or regional syntheses.

Economic skarn deposits can be subdivided into several main types, based upon the dominant contained metal (*e.g.*, W, Fe, Cu, *etc.*). This is similar to the classification of porphyry deposits into porphyry copper,
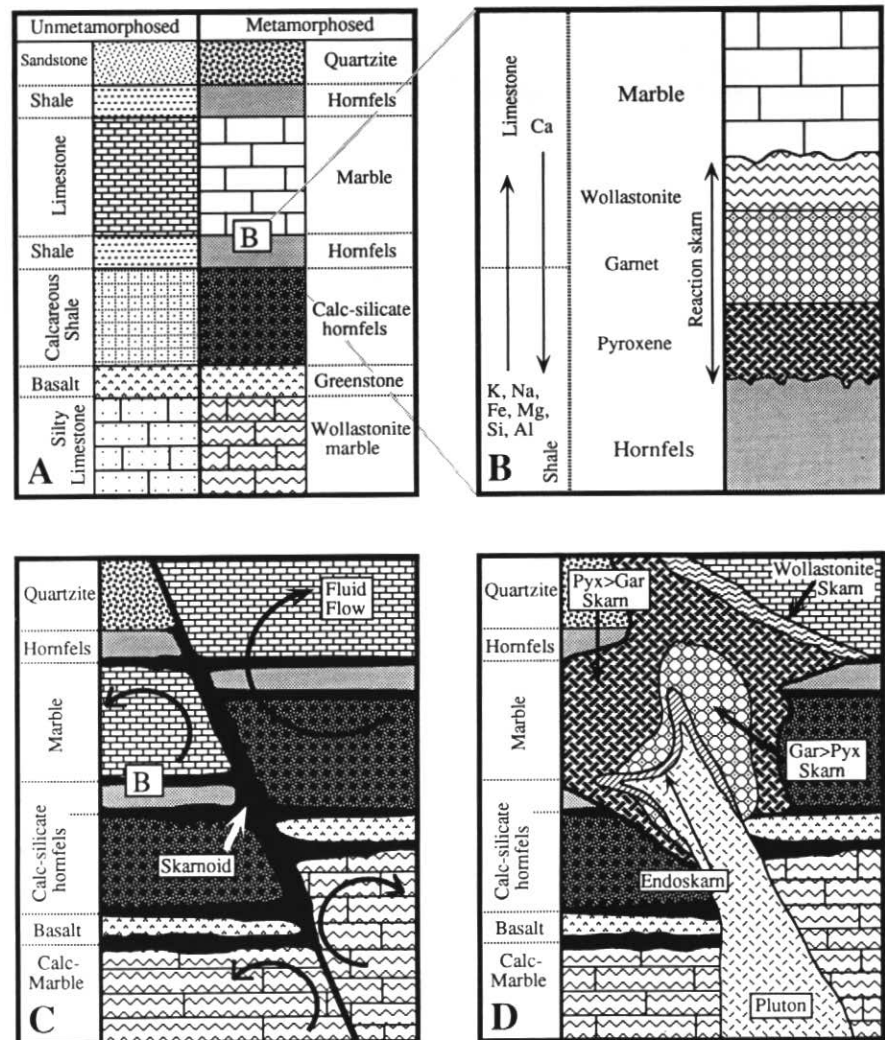
Figure 1 *Types of skarn formation:* (**A**) *Isochemical metamorphism involves recrystallization and changes in mineral stability without significant mass transfer;* (**B**) *Reaction skarn results from metamorphism of interlayered lithologies, such as shale and limestone, with mass transfer between layers on a small scale (bimetasomatism);* (**C**) *Skarnoid results from metamorphism of impure lithologies with some mass transfer by small-scale fluid movement;* (**D**) *Fluid-controlled metasomatic skarn typically is coarse grained and does not closely reflect the composition or texture of the protolith.*

porphyry molybdenum, and porphyry tin types; these deposits share many alteration and geochemical features, but are, nevertheless, easily distinguishable. In order to explore for economically viable skarn deposits, it is necessary to understand the typical characteristics of each skarn group and the differences among them. The purpose of this paper is to develop a useful exploration model based upon the typical characteristics of skarns in general, and the various deposit types in particular. There have been numerous general review papers on skarn deposits in the past few decades (e.g., Watanabe, 1960; Phan, 1969; Zharikov, 1970; Smirnov, 1976; Burt, 1977; Einaudi et al., 1981; Meinert, 1983; Ray and Webster, 1991a) and the reader is referred to these sources for more detailed considerations of skarn terminology and genesis.

DEFINITIONS AND TERMINOLOGY

Skarn deposits have been described in the scientific literature since at least the 19th century (e.g., Cotta, 1864). The term "skarn" originated in Sweden as a mining term used to describe the relatively coarse-grained, calc-silicate gangue associated with some iron ores (Geijer and Magnusson, 1952). Burt (1982) provides an interesting historical account of the subsequent evolution of skarn terminology and wisely notes that most attempts to include genetic concepts in formal definitions have created additional problems and confusion. Most modern authors have adopted Einaudi et al.'s (1981) suggestion to use skarn and skarn deposit as descriptive terms based upon their contained mineralogy, free of genetic implications.

Not all skarns have economic mineralization; those which do are called skarn deposits. In most large skarn deposits, skarn and ore minerals result from the same hydrothermal system, even though there may be significant differences in the time/space distribution of these minerals on a local scale. Although rare, it is also possible to form skarn by metamorphism of pre-existing ore deposits, as has been suggested for Aguilar in Argentina (Gemmell et al., 1992), Franklin Furnace in the United States (Johnson et al., 1990), and Broken Hill in Australia (Hodgson, 1975).

Skarns can be subdivided according to several criteria. Exoskarn and endoskarn are common terms used to indicate a sedimentary and igneous protolith, respectively. Magnesian and calcic skarn can be used to describe the dominant composition of the protolith and resulting skarn minerals. Such terms can be combined, as in the case of a magnesian exoskarn, which contains forsterite-diopside skarn formed from dolostone. Calc-silicate hornfels is a descriptive term often used for the relatively fine-grained, calc-silicate rocks that result from metamorphism of impure carbonate units such as silty limestone or calcareous shale

(Fig. 1A). Reaction skarns (Fig. 1B) can form from isochemical metamorphism of thinly interlayered shale and carbonate units, where metasomatic transfer of components between adjacent lithologies may occur on a small scale (perhaps centimetres) (e.g., Vidale, 1969; Zarayskiy et al., 1987). Skarnoid (Fig. 1C) is a descriptive term for calc-silicate rocks which are relatively fine grained, iron poor, and which reflect, at least in part, the compositional control of the protolith (Korzkinskii, 1948; Zharikov, 1970). Genetically, skarnoid is intermediate between a purely metamorphic hornfels and a purely metasomatic, coarse-grained skarn (sometimes termed infiltration skarn). For all of the preceding terms, the composition and texture of the protolith tend to control the composition and texture of the resulting skarn. In contrast, most economically important skarn deposits result from large-scale metasomatic transfer, where fluid composition controls the resulting skarn and ore mineralogy (Fig. 1D). Even though many of these terms are fairly specific, there is a continuum, both conceptually and in the field, between purely metamorphic and purely metasomatic processes (e.g., Hietanen, 1962; Newberry, 1991).

EVOLUTION OF SKARN DEPOSITS

As was recognized by early skarn researchers (e.g., Lindgren 1902; Barrell, 1907; Goldschmidt, 1911; Umpleby, 1913; Knopf,

1918), formation of a skarn deposit is a dynamic process. In most large skarn deposits, there is a transition from early/distal metamorphism resulting in hornfels, reaction skarn, and skarnoid, to later/proximal metasomatism resulting in relatively coarse-grained, ore-bearing skarn. Due to the strong temperature gradients and large fluid circulation cells caused by intrusion of a magma (Norton, 1982; Salemink and Schuiling, 1987; Bowers et al., 1990), contact metamorphism can be considerably more complex than the simple model of isochemical recrystallization typically invoked for regional metamorphism. Figure 2 illustrates the effects of circulating diverse fluids through a fracture in a relatively simple carbonate protolith. The resulting vein-controlled skarn mineralogy in Figures 2B and 2C could easily be mistaken for the product of prograde metasomatism, even though it involves pure water, and the fluid in Figure 2C is actually cooler than the surrounding rock. Circulation of such fluids by the steep thermal gradients common in most plutonic environments results in complex metamorphic aureoles, complete with small-scale metasomatic transfer (Fig. 1B). More complex metasomatic fluids, with the possible addition of magmatic components such as Fe, Si and Cu (Fig. 2D), produce a continuum between purely metamorphic and purely metasomatic processes.

This early metamorphism and continued metasomatism at relatively high tempera-
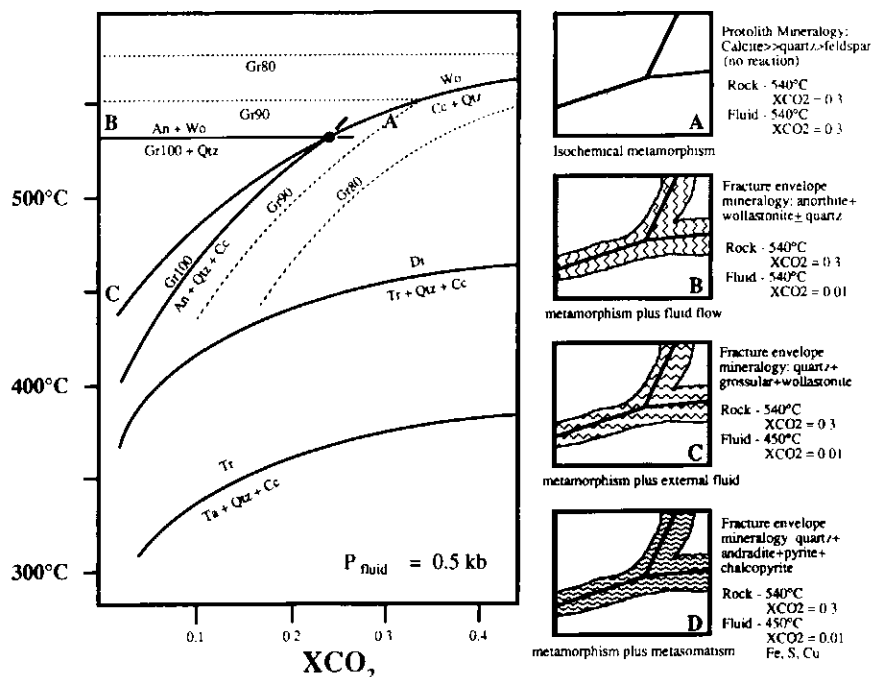
Figure 2 Illustration of metamorphic phase equilibria for selected reactions in the system Ca-Mg-Al-Si-H_2O-CO_2. Modified from Greenwood (1967) and Kerrick (1974). Examples of four fracture-controlled alteration events are illustrated: (A) Fluid in fracture is same temperature and composition as surrounding rocks at high XCO_2; (B) Fluid in fracture is same temperature as surrounding rocks but has flushed some CO_2 out of the system; (C) Fluid in fracture is cooler than surrounding rocks and has flushed some CO_2 out of the system; (D) Fluid in fracture is a concentrated metasomatic fluid with magmatic components including Fe, Cu and S. Cc = calcite; Ta = talc; other abbreviations as in Table 1.

tures (Wallmach and Hatton (1989) describe temperatures >1200°C) are followed by retrograde alteration as temperatures decline. A link between space and time is a common theme in ore deposits and requires careful interpretation of features which may appear to occur only in a particular place (*e.g.*, Barton *et al.*, 1991). For skarns related to plutons, there is a parallel relationship between the sequence of emplacement, crystallization, alteration and cooling of the pluton and the corresponding metamorphism, metasomatism and retrograde alteration in the surrounding rocks.

Figure 3 illustrates the general sequence of skarn development for such pluton-related systems. The degree to which a particular stage is developed in a specific skarn will depend on the local geologic environment of formation. For example, metamorphism will likely be more extensive and of higher grade around a skarn formed at relatively great crustal depth than one formed under shallower conditions (Fig. 3C). Conversely, retrograde alteration during cooling, and possible interaction with meteoric water, will be more intense in a skarn formed at relatively shallow depths in the earth's crust compared with one formed at greater depths (Fig. 3D). In the deeper skarns, carbonate rocks may deform in a ductile manner rather than through brittle fracture, with bedding parallel to the intrusive contact; in shallower systems the reverse may be true. These differences in structural style will, in turn, affect the size and morphology of skarn. Thus, host rock composition, depth of formation, and structural setting will all cause variations from the idealized pluton-associated skarn model of Figure 3. The nature of these variations with respect to individual skarn deposits is considered in more detail in later sections.

SKARN MINERALOGY

The identification and classification of skarn deposits is based on their mineralogy. Although many skarn minerals are typical rock-forming minerals, some are less abundant and most have compositional variations that can yield significant information about the environment of formation. Table 1 lists many of the common skarn minerals and their end-member compositions. Some minerals, such as quartz and calcite, are present in almost all skarns. Others, such as humite, periclase, phlogopite, talc, serpentine and brucite, are typical of magnesian skarns, but are absent from most other skarn types. Additionally, there are many tin, boron, beryllium and fluorine-bearing minerals which have very restricted, but locally important, parageneses.

Modern analytical techniques, particularly the electron microprobe, make it relatively easy to determine accurate mineral compositions and, consequently, to use precise mineralogical names. However, mineralogical names should be used correctly, so as not to imply more than is known about the mineral composition. For example, the sequence pyroxene-clinopyroxene-calcic clinopyroxene-diopsidic pyroxene-diopside comprises increasingly more specific terms. Unfortunately, it is all too common in the geologic literature for specific end-member terms, such as diopside, to be used when all that is known about the mineral in question is that it might be pyroxene.

Zharikov (1970) was perhaps the first to describe systematic variations in skarn mineralogy among the major skarn classes. He used phase equilibria, mineral compatibilities, and compositional variations in solid solution series to describe and predict characteristic mineral assemblages for different skarn types. His observations have been extended by Burt (1972) and Einaudi *et al.* (1981) to include a wide variety of deposit types and the mineralogical variations between types. The minerals which are most useful for both classification and exploration are those, such as garnet, pyroxene and amphibole, which are present in all skarn types and which show marked compositional variability. For example, the manganiferous pyroxene, johannsenite, is found almost exclusively in zinc skarns. Its presence, without much supporting information, is definitive of this skarn type. When compositional information is available, it is possible to denote a mineral's composition in terms of mole % of the end members. For example, a pyroxene which contains 70 mole % hedenbergite, 28 mole % diopside, and 2 mole % johannsenite could be referred to as
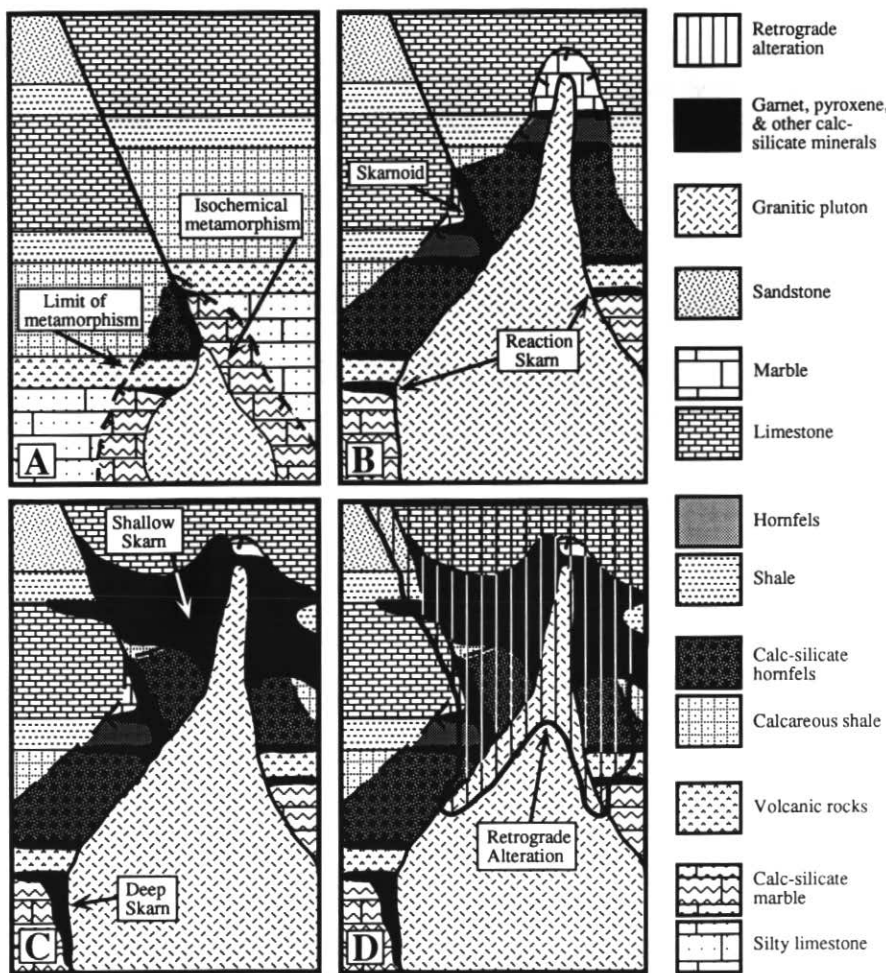
Figure 3 *Evolutionary stages of pluton-associated skarn deposits:* **(A)** *Initial intrusion causes metamorphism of sedimentary rocks.* **(B)** *Metamorphic recrystallization and phase changes reflect protolith compositions, with local bimetasomatism and fluid circulation forming diverse calc-silicate minerals (reaction skarns and skarnoid) in impure lithologies and along fluid boundaries. Note that metamorphism is more extensive and higher in temperature at depth than adjacent to the small cupola near the top of the system.* **(C)** *Crystallization and release of a separate aqueous phase result in fluid-controlled metasomatic skarn. Note that skarn at depth is small relative to the size of the metamorphic aureole. It is also vertically oriented compared to the laterally extensive skarn which locally extends beyond the metamorphic aureole near the top of the system.* **(D)** *Cooling of the pluton and the possible circulation of cooler, oxygenated meteoric waters cause retrograde alteration of metamorphic and metasomatic calc-silicate assemblages. Note that retrograde alteration is more extensive in shallow zones.*

$Hd_{70}Di_{28}Jo_2$. In many skarn systems, variation in iron content is the most important parameter and, thus, many minerals are described simply by their iron end member, e.g., Hd_{10} or Ad_{90} (Table 1).

Large amounts of compositional information can be summarized graphically. Triangular plots commonly are used to express variations in compositionally complex minerals such as garnet and pyroxene (Fig. 4). Amphiboles are more difficult to portray graphically because they have structural as well as compositional variations. The main differences between amphiboles in different skarn types are variations in the amounts of Fe, Mg, Mn, Ca, Al, Na and K. Amphiboles in Au, W and Sn skarns are progressively more aluminous (actinolite-hastingsite-hornblende); amphiboles in Cu, Mo and Fe skarns are progressively more iron rich in the tremolite-actinolite series; and amphiboles in zinc skarns are both Mn rich and Ca deficient, ranging from actinolite to dannemorite. For a specific skarn deposit or group of skarns, compositional variations in less common mineral phases, such as vesuvianite, bustamite and olivine, may provide insight into zonation patterns or regional petrogenesis (e.g., Giere, 1986; Agrell and Charnely, 1987; Silva and Siriwardena, 1988; Benkerrou and Fonteilles, 1989).

The spatial and temporal arrangement of minerals in skarn deposits has long been a focus of study. As noted by Burt (1977), European researchers typically have emphasized spatial mineral zoning, whereas North American researchers have emphasized temporal mineral zoning in skarn deposits. Both types of zoning occur in skarns, and their superposition creates the characteristically complex patterns illustrated in Figure 3. In most skarns, there is a general zonation pattern of proximal garnet, distal pyroxene, and vesuvianite (or a pyroxenoid such as wollastonite, bustamite or rhodonite) at the contact between skarn and marble. In addition, individ- ual skarn minerals may display systematic colour or compositional variations within the larger zonation pattern. For example, garnet is commonly dark red-brown in proximal occurrences, becomes lighter brown in more distal occurrences, and is pale green near the marble front (e.g., Atkinson and Einaudi, 1978). The change in pyroxene colour is less pronounced, but typically reflects a progressive increase in iron and/or manganese toward the marble front (e.g., Harris and Einaudi, 1982). For some skarn systems, these zonation patterns can be "stretched out" for several kilometres and can provide a significant exploration guide (e.g., Meinert, 1987).

Retrograde skarn mineralogy, in the form of epidote, amphibole, chlorite and other hydrous phases, is typically structurally controlled and overprints the prograde zonation sequence. Thus, there is often a zone of abundant hydrous minerals along fault, stratigraphic or intrusive contacts. This su-

Table 1   Skarn mineralogy — common minerals, mineral groups, abbreviations and compositions.

General Group	End Members	Abbreviation	Composition		Series
Garnet	grossularite	Gr	$Ca_3Al_2(SiO_4)_3$	}	grandite
	andradite	Ad	$Ca_3Fe_2(SiO_4)_3$		
	spessartine	Sp	$Mn_3Al_2(SiO_4)_3$	}	sub-calcic garnet
	almandine	Al	$Fe_3Al_2(SiO_4)_3$		
	pyrope	Py	$Mg_3Al_2(SiO_4)_3$		
Pyroxene	diopside	Di	$CaMgSi_2O_6$	}	salite
	hedenbergite	Hd	$CaFeSi_2O_6$		
	johannsenite	Jo	$CaMnSi_2O_6$		
	fassaite	Fas	$Ca(Mg,Fe,Al)(Si,Al)_2O_6$		
Olivine	larnite	Ln	Ca_2SiO_4	}	monticellite
	forsterite	Fo	Mg_2SiO_4		
	fayalite	Fa	Fe_2SiO_4	}	knebelite
	tephroite	Tp	Mn_2SiO_4		
Pyroxenoid	ferrosilite	Fs	$FeSiO_3$	}	pyroxemangite
	rhodonite	Rd	$MnSiO_3$		
	wollastonite	Wo	$CaSiO_3$		bustamite
Amphibole	tremolite	Tr	$Ca_2Mg_5Si_8O_{22}(OH)_2$	}	actinolite
	ferroactinolite	Ft	$Ca_2Fe_5Si_8O_{22}(OH)_2$		
	manganese actinolite	Ma	$Ca_2Mn_5Si_8O_{22}(OH)_2$		
	hornblende	Hb	$Ca_2(Mg,Fe)_4Al_2Si_7O_{22}(OH)_2$		
	pargasite	Pg	$NaCa_2(Mg,Fe)_4Al_3Si_6O_{22}(OH)_2$		
	cummingtonite	Cm	$Mg_2(Mg,Fe)_5Si_8O_{22}(OH)_2$		
	dannemorite	Dm	$Mn_2(Fe,Mg)_5Si_8O_{22}(OH)_2$	}	sub-calcic amphibole
	grunerite	Gru	$Fe_2(Fe,Mg)_5Si_8O_{22}(OH)_2$		
Epidote	piemontite	Pm	$Ca_2(Mn,Fe,Al)_3(SiO_4)_3(OH)$		
	allanite	All	$(Ca,REE)_2(Fe,Al)_3(SiO_4)_3(OH)$		
	epidote	Ep	$Ca_2(Fe,Al)_3(SiO_4)_3(OH)$		
	clinozoisite	Cz	$Ca_2Al_3(SiO_4)_3(OH)$		
Plagioclase	anorthite	An	$CaAl_2Si_2O_8$		
Scapolite	marialite	Ml	$Na_4Al_3Si_9O_{24}(Cl,CO_3,OH,SO_4)$		
	meionite	Me	$Ca_4Al_3Si_6O_{24}(CO_3,Cl,OH,SO_4)$		
Axinite		Ax	$(Ca,Mn,Fe,Mg)_3Al_2BSi_4O_{15}(OH)$		
Other	vesuvianite (idocrase)	Vs	$Ca_{10}(Mg,Fe,Mn)_2Al_4Si_9O_{34}(OH,Cl,F)_4$		
	prehnite	Pr	$Ca_2Al_2Si_3O_{10}(OH)_2$		

perposition of later phases can be difficult to discriminate from a spatial zonation sequence due to progressive reaction of a metasomatic fluid. It is important to realize that hydrous minerals do not necessarily represent retrograde alteration (*e.g.*, Dick and Hodgson, 1982). For example, the typically high-fluorine activities in tin skarns can stabilize many hydrous minerals at high temperatures during early skarn alteration stages (*e.g.*, Lost River in Alaska; Dobson, 1982). In general, retrograde alteration is more intense and more pervasive in shallower skarn systems. In some shallow, porphyry copper-related skarn systems, extensive retrograde alteration almost completely obliterates the prograde garnet and pyroxene (Einaudi, 1982a, 1982b).

DEPTH OF FORMATION
One of the more fundamental controls on skarn size, geometry and style of alteration is the depth of formation. Quantitative geobarometric studies typically use mineral equilibria (Anovitz and Essene, 1990), fluid inclusions (Guy *et al.*, 1988), or a combination of these methods (Hames *et al.*, 1989) to estimate the depth of metamorphism. Qualitative methods include stratigraphic or other geologic reconstructions and interpretation

of igneous textures. Simple observations of chilled margins, grain size of porphyry groundmass, pluton morphology, and presence of brecciation and brittle fracture allow field distinctions between relatively shallow and deeper environments. The effect of depth on metamorphism is largely a function of the ambient wall rock temperature prior to, during and after intrusion. Assuming an average geothermal gradient for an orogenic zone of approximately 35°C per kilometre (Blackwell *et al.*, 1990), the ambient wall rock temperature prior to intrusion at 2 km would be 70°C, whereas at 12 km it would be 420°C. Thus, with the added heat flux provided by local igneous activity, the volume of rock affected by temperatures in the 400-700°C range would be considerably larger, and the effects longer lived, surrounding a deeper skarn than a shallower one. In addition, higher ambient temperatures could affect the crystallization history of a pluton and minimize the amount of retrograde alteration of skarn minerals. At a depth of 12 km, with ambient temperatures of approximately 400°C, skarn may not cool below garnet and pyroxene stability without subsequent uplift or other tectonic changes.

The greater extent and intensity of metamorphism at depth can affect the permea-

bility of host rocks and reduce the amount of carbonate available for reaction with metasomatic fluids. An extreme case is described by Dick and Hodgson (1982) at CanTung in Canada, where the "Swiss cheese limestone" was almost entirely converted to a heterogeneous, calc-silicate hornfels during metamorphism prior to skarn formation. The skarn formed from the few remaining patches of limestone has some of the highest known grades of tungsten skarn ore in the world (Mathieson and Clark, 1984).

The depth of skarn formation also will affect the mechanical properties of the host rocks. In a deep skarn environment, rocks will tend to deform in a ductile manner, rather than fracture. Intrusive contacts with sedimentary rocks at depth tend to be sub-parallel to bedding; either the pluton intrudes along bedding planes or the sedimentary rocks fold or flow until they are aligned with the intrusive contact. Examples of skarns for which depth estimates exceed 5-10 km include Pine Creek in California (Brown *et al.*, 1985) and Osgood Mountains in Nevada (Taylor, 1976). In occurrences such as these, where intrusive contacts are sub-parallel to bedding planes, skarn is usually confined to a narrow, but vertically extensive, zone. At Pine Creek, skarn is typically <10 m wide, but locally exceeds 1 km in length and vertical extent (Newberry, 1982). Thus, skarn formed at greater depths (Fig. 3C) can be seen as a narrow rind of small size relative to the associated pluton and its metamorphic aureole.

In contrast, host rocks at shallow depths will tend to deform by fracturing and faulting rather than folding. In most of the 13 relatively shallow skarn deposits reviewed by Einaudi (1982a), intrusive contacts are sharply discordant to bedding, and skarn cuts across bedding and massively replaces favourable beds, equalling or exceeding the (exposed) size of the associated pluton. The strong hydrofracturing associated with shallow intrusions greatly increases the permeability of the host rocks, not only for igneous-related metasomatic fluids, but also for later, possibly cooler, meteoric fluids (Shelton, 1983). The influx of meteoric water and the consequent destruction of skarn minerals during retrograde alteration is one of the distinctive features of skarn formation in a shallow environment.

The shallowest (and youngest) known skarns are presently forming in active geothermal systems (McDowell and Elders, 1980; Cavarretta *et al.*, 1982; Bird *et al.*, 1984; Cavarretta and Puxeddu, 1990) and hot spring vents on the sea floor (Zierenberg and Shanks, 1983). These skarns represent the distal expression of magmatic activity; exposed igneous rocks (in drill core) are dominantly thin dykes and sills with chilled margins and a very fine-grained to aphanitic groundmass.
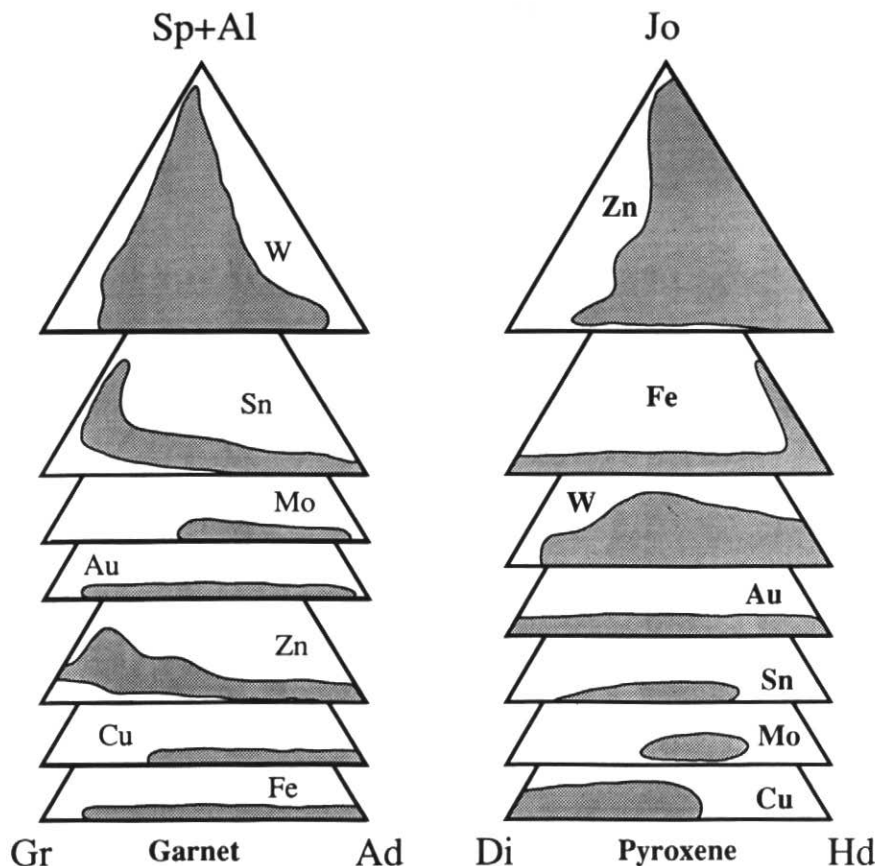
Figure 4   *Ternary plots of garnet and pyroxene compositions from major skarn types. End members are: Ad = andradite, Gr = grossularite, Al = almandine, Sp = spessartine, Hd = hedenbergite, Di = diopside, Jo = johannsenite. Data from Einaudi et al. (1981) and Meinert (1983, 1989).*

GENERAL CHARACTERISTICS OF IMPORTANT SKARN DEPOSIT TYPES

Groupings of skarn deposits can be based on descriptive features such as protolith composition, rock type, and dominant economic metal(s), as well as genetic features such as mechanism of fluid movement, temperature of formation, and extent of magmatic involvement. The general trend of modern authors is to adopt a descriptive skarn classification based upon the dominant economic metals, and then to modify individual categories based upon compositional, tectonic or genetic variations. Seven major skarn types (Fe, Au, W, Cu, Zn, Mo and Sn) have received significant modern study, and several others (including F, C, Ba, Pt, U and REE) are locally important. Table 2 summarizes the general characteristics of selected examples of the major skarn deposit types. More detailed descriptions and maps of individual skarn deposits are presented in the references cited and will not be repeated here.

Iron Skarns

The largest skarn deposits are the iron skarns. Major reviews of this deposit type include Sangster (1969), Sokolov and Grigorev (1977), and Einaudi et al. (1981). Iron skarns are mined for their magnetite content and, although minor amounts of Cu, Co, Ni and Au may be present, iron is typically the only commodity recovered (Grigoryev et al., 1990). Many deposits are very large (>500 million tons, with >300 million tons contained Fe) and consist dominantly of magnetite, with only minor silicate gangue. Some deposits contain significant amounts of copper and are transitional to more typical copper skarns (e.g., Kesler, 1968; Vidal et al., 1990). Calcic iron skarns in oceanic island arcs are associated with iron-rich plutons intruded into limestone and volcanic wall rocks. In some deposits, the amount of endoskarn may exceed exoskarn. Skarn minerals consist dominantly of garnet and pyroxene, with lesser epidote, ilvaite and actinolite; all are iron rich (Purtov et al., 1989). Alteration of igneous rocks is common, with widespread albite, orthoclase and scapolite veins and replacements, in addition to endoskarn. In contrast, magnesian iron skarns are associated with diverse plutons in a variety of tectonic settings; the unifying feature is that they all form from dolomitic wall rocks. In magnesian skarns, the main skarn minerals, such as forsterite, diopside, periclase, talc and serpentine, do not contain much iron. Thus, the available iron in solution tends to form magnetite rather than andradite or hedenbergite (e.g., Hall et al., 1988). Overprinting of calcic skarn upon magnesian skarn is reported from many Russian deposits (Sokolov and Grigorev, 1977; Aksyuk and Zharikov, 1988). In addition, many other skarn types contain pockets of massive magnetite which may be mined for iron on a local scale (e.g., Fierro area in New Mexico; Her-

non and Jones, 1968). Most of these occurrences form from dolomitic strata or from zones that have experienced prior magnesian metasomatism (e.g., Imai and Yamazaki, 1967).

Gold Skarns

Although gold skarns had been mined since the late 1800s (Hedley district in British Columbia; Billingsley and Hume, 1941), there was so little published about them until recently that they were not included in the major world review of skarn deposits by Einaudi et al. (1981). In the past decade, multiple gold skarn discoveries have prompted new scientific studies and several overview papers, the most recent and comprehensive of which is Theodore et al. (1991). The highest-grade (5-15 g/t Au) gold skarn deposits (e.g., Hedley district; Ettlinger, 1990; Ettlinger et al., 1992; Fortitude in Nevada; Myers and Meinert, 1991) are relatively reduced, are mined solely for their precious metal content, and lack economic concentrations of base metals. Other gold skarns (e.g., McCoy in Nevada; Brooks et al., 1991) are more oxidized, have lower gold grades (1-5 g/t Au) and contain subeconomic amounts of other metals such as Cu, Pb and Zn. Several other skarn types, particularly Cu skarns, contain enough gold (0.01->1 g/t Au) for it to be a by-product. A few skarn deposits, although having economic base metal grades, are being mined solely for their gold content (e.g., Veselyi Mine in the Commonwealth of Independent States, Ettlinger and Meinert, 1991). Most high-grade gold skarns are associated with reduced (ilmenite-bearing, Fe^{3+}/Fe^{2+} <0.75), diorite-granodiorite plutons and dyke/sill complexes. Such skarns are dominated by iron-rich pyroxene (typically >Hd_{50}); proximal zones can contain abundant intermediate grandite garnet. Other common minerals include potassium feldspar, scapolite, vesuvianite, apatite and high-chlorine aluminous amphibole. Distal/early zones contain biotite ± potassium feldspar hornfels which can extend for hundreds of metres beyond massive skarn. Due to the clastic-rich, carbonaceous nature of the sedimentary rocks in these deposits, most skarn is relatively fine grained. Some gold skarns contain unusual late prehnite or wollastonite retrograde alteration (Ettlinger, 1990). Arsenopyrite and pyrrhotite are the dominant sulphide minerals at Hedley and Fortitude, respectively. Most gold is present as electrum and is strongly associated with various bismuth and telluride minerals, including native bismuth, hedleyite, wittichenite and maldonite. The Fortitude deposit is part of a large zoned skarn system in which the proximal, garnet-rich part was mined for copper (Theodore and Blake, 1978). Similarly, the Crown Jewel gold skarn in Washington is the pyroxene-rich, distal portion of a large skarn system in which the proximal part is garnet

rich and was mined on a small scale for iron and copper (Hickey, 1990). Such zoned skarn systems suggest that other skarn types may have undiscovered precious metal potential if the entire skarn system has not been explored (e.g., Soler et al., 1990).

Tungsten Skarns

Tungsten skarns are found on most continents, in association with calc-alkalic plutons in major orogenic belts. Major reviews of tungsten skarns include Newberry and Einaudi (1981), Newberry and Swanson (1986), and Kwak (1987). As a group, tungsten skarns are associated with coarse-grained, equigranular batholiths (with pegmatite and aplite dykes) surrounded by large, high-temperature, metamorphic aureoles. These features are collectively indicative of a deep environment. Plutons are typically fresh, with only minor myrmekite and plagioclase-pyroxene endoskarn zones near contacts. The high-temperature metamorphic aureoles common in the tungsten skarn environment contain abundant calc-silicate hornfels and skarnoid formed from mixed carbonate-pelite sequences (e.g., Figs. 1A-C and 2C). Such metamorphic calc-silicate minerals reflect the composition and texture of the protolith and can be distinguished from ore-grade metasomatic skarn in the field and in the laboratory.

Newberry and Einaudi (1981) divided tungsten skarns into reduced and oxidized types, based on host rock composition (carbonaceous versus hematitic), skarn mineralogy (ferrous versus ferric iron), and relative depth (metamorphic temperature and involvement of oxygenated ground water). Early skarn assemblages in reduced tungsten skarns are dominated by hedenbergitic pyroxene and lesser grandite garnet, with associated disseminated, fine-grained, molybdenum-rich scheelite (powellite). Later garnets are subcalcic (Newberry, 1983) with significant amounts (up to 80 mole %) of spessartine and almandine. This subcalcic garnet is associated with leaching of early disseminated scheelite and its redeposition as coarse-grained, often vein-controlled, low-molybdenum scheelite. It is also associated with the introduction of sulphides, such as pyrrhotite, molybdenite, chalcopyrite, sphalerite and arsenopyrite, and hydrous minerals such as biotite, hornblende and epidote. In oxidized tungsten skarns, andraditic garnet is more abundant than pyroxene, scheelite is molybdenum poor, and ferric iron phases are more common than ferrous phases. For example, at the Springer deposit in Nevada, garnet is abundant and has andraditic rims, pyroxene is diopsidic (<Hd_{40}), epidote is the dominant hydrous mineral, pyrite is more common than pyrrhotite, and subcalcic garnet is rare to absent (Johnson and Keith, 1991). In general, oxidized tungsten skarns tend to be smaller than reduced tungsten skarns, although the

highest grades in both systems typically are associated with hydrous minerals and retrograde alteration.

Copper Skarns

Copper skarns are perhaps the world's most abundant skarn type. They are particularly common in orogenic zones related to subduction, both in oceanic and continental settings. Major reviews of copper skarns include Einaudi et al. (1981) and Einaudi (1982a, 1982b). Most copper skarns are associated with I-type, magnetite series, calc-alkalic, porphyritic plutons, many of which have cogenetic volcanic rocks, stockwork veining, brittle fracturing and brecciation, and intense hydrothermal alteration. These are all features indicative of a relatively shallow environment of formation.

Most copper skarns form in close proximity to the contacts of stocks, with a relatively oxidized skarn mineralogy dominated by andraditic garnet. Other phases include diopsidic pyroxene, vesuvianite, wollastonite, actinolite and epidote. Hematite and magnetite are common in most deposits, and the presence of dolomitic wall rocks is coincident with massive magnetite lodes, which may be mined on a local scale for iron. As noted by Einaudi et al. (1981), copper skarns commonly are zoned, with massive garnetite near the pluton, increasing pyroxene away from the contact, and, finally, vesuvianite and/or wollastonite occurring near the marble contact. In addition, garnet may be colour zoned from dark reddish-brown proximal to the pluton, to green and yellow varieties in distal occurrences. Sulphide mineralogy and metal ratios may also be systematically zoned relative to the causative pluton. In general, pyrite and chalcopyrite are most abundant near the pluton, with chalcopyrite increasing away from the pluton, and bornite finally occurring in wollastonite zones near the marble contact. In copper skarns containing monticellite (e.g., Ertsberg, Irian Jaya in Indonesia; Kyle et al., 1991, and Maid of Erin in British Columbia; Meinert, unpub. data), bornite-chalcocite are the dominant Cu-Fe sulphides, rather than pyrite-chalcopyrite.

The largest copper skarns are associated with mineralized porphyry copper plutons. These deposits can exceed 1 billion tons of combined porphyry and skarn ore, with more than 5 million tons of copper recoverable from skarn. The mineralized plutons exhibit characteristic potassium silicate and sericitic alteration, which can be correlated with prograde garnet-pyroxene and retrograde epidote-actinolite, respectively, in the skarn. Intense retrograde alteration is common in copper skarns and may destroy most of the prograde garnet and pyroxene in some porphyry-related deposits (e.g., Ely in Nevada; James, 1976). Endoskarn alteration of mineralized plutons is rare. In contrast, barren stocks associated with copper skarns contain abundant epidote-actinolite-chlorite en-

doskarn and less intense retrograde alteration of skarn. Some copper deposits have coarse-grained actinolite-chalcopyrite-pyrite-magnetite ores, but contain only sparse prograde garnet-pyroxene skarn (e.g., Monterrosas and Raúl-Condestable deposits in Peru (Ripley and Ohmoto, 1977; Sidder, 1984; Vidal et al., 1990); Record mine in Oregon (Caffrey, 1982); and Cerro de Mercado in Mexico (Lyons, 1988)). These deposits provide a link between some copper and iron skarns and deposits with volcanogenic and orthomagmatic affinities.

Zinc skarns

Most zinc skarns occur in continental settings associated with either subduction or rifting. They are mined for ores of zinc, lead and silver, although zinc is usually dominant. They are also high grade (10-20% Zn + Pb, 30-300 g/t Ag). Related igneous rocks span a wide range of compositions, from diorite through high-silica granite. They also span diverse geological environments, from deep-seated batholiths to shallow dyke-sill complexes to surface volcanic extrusions. The common thread linking most zinc skarn ores is their occurrence distal to associated igneous rocks. Major reviews of zinc skarn deposits include Einaudi et al. (1981) and Megaw et al. (1988).

Zinc skarns can be subdivided according to several criteria, including distance from magmatic source, temperature of formation, relative proportion of skarn and sulphide minerals, and geometric shape of the ore body. None of these criteria is entirely satisfactory: a magmatic source cannot be identified for some deposits, most skarns develop over a range of temperatures, and most large skarn deposits contain both skarn-rich and skarn-poor ores in a variety of geometric settings, including mantos and chimneys. Megaw et al. (1988) make the important point that many zinc skarn districts, "*grade outward from intrusion-associated mineralization to intrusion-free ores, which suggests that those districts lacking known intrusion relationships may not have been traced to their ends*". Similarly, most zinc skarn districts grade outward from skarn-rich mineralization to skarn-poor ores, veins and massive sulphide bodies, which may contain few, if any, skarn minerals. Incompletely explored districts may have only some of these zones exposed. As previously noted, however, the presence within the system of skarn minerals, such as garnet and pyroxene, is important because it indicates a restricted geochemical environment which is entirely distinct from other ore types, such as Mississippi Valley-type deposits, which also contain Zn-Pb-Ag ores, but which absolutely lack skarn minerals.

Besides their Zn-Pb-Ag metal content, zinc skarns can be distinguished from other skarn types by their distinctive manganese- and iron-rich mineralogy, by their occurrence

along structural and lithologic contacts, and by the absence of significant metamorphic aureoles centered on the skarn. Almost all skarn minerals in these deposits can be enriched in manganese, including garnet, pyroxene, olivine, ilvaite, pyroxenoid, amphibole, chlorite and serpentine. In some deposits, the pyroxene:garnet ratio and the manganese content of pyroxene increase systematically along the fluid flow path (e.g., Groundhog in New Mexico; Meinert, 1987). This feature has been used to identify proximal and distal skarns and proximal and distal zones within individual skarn deposits. The occurrence of zinc skarns in distal portions of major magmatic/hydrothermal systems may make even small deposits potentially useful as exploration guides in poorly exposed districts. Thus, reports of manganese-rich mineral occurrences may provide clues to districts that have not yet received significant exploration activity.

Molybdenum Skarns

Most molybdenum skarns are associated with leucocratic granites, and range from high-grade, relatively small deposits (Azegour in Morocco; Permingeat, 1957) to low-grade, bulk tonnage deposits (Little Boulder Creek in Idaho; Cavanaugh, 1978). Numerous small occurrences are also found in Precambrian, stable cratons associated with pegmatite, aplite and other leucocratic rocks (Vokes, 1963). Most molybdenum skarns contain a variety of metals, including W, Cu, Zn, Pb, Bi, Sn and U, and some are truly polymetallic, in that several metals need to be recovered together in order for the deposits to be mined economically. Mo-W-Cu is the most common association, and some tungsten skarns and copper skarns contain zones of recoverable molybdenum. Most molybdenum skarns occur in silty carbonate or calcareous clastic rocks; Cannivan Gulch in Montana (Darling, 1990) is a notable exception in that it occurs in dolomite. Hedenbergitic pyroxene is the most common calc-silicate mineral reported from molybdenum skarns, with lesser grandite garnet (with minor pyralspite component), wollastonite, amphibole and fluorite. This skarn mineralogy indicates a reducing environment with high fluorine activities. These deposits have not received significant study outside of the former Soviet Union and there has not been a modern review since the brief summary by Einaudi et al. (1981).

Tin Skarns

Tin skarns are almost exclusively associated with high-silica granites generated by partial melting of continental crust, usually caused by rifting events. Major reviews of tin skarn deposits include Einaudi et al. (1981) and Kwak (1987). Tin skarns can be subdivided according to several criteria, including proximal *versus* distal, calcic *versus* magnesian, skarn-rich *versus* skarn-poor, oxide-rich *ver-*

Table 2   General characteristics of major skarn deposit types.

Skarn Type	Name and Location	Tonnage and Grade	Tectonic Setting	Pluton and Alteration	Protolith	Skarn Mineralogy	Ore Mineralogy	Geochemistry	References
Magnesian Iron	Mojave Desert Region, Eagle Mountain, Iron Hat Mine, California, USA	EM: >50 Mt 45% Fe; IH: 0.2 Mt 59% Fe; total S < 0.03%	Continental subduction	165 Ma alkali feldspar granite stock with albitic alteration and granitic dyke swarm with ep endoskarn	Paleozoic dolomite >> limestone, shale, sandstone	forsterite, periclase, clinohumite > ph, serp, talc pyx(Hd10-70, Jo<2) gar(Ad30-95), wo, ep, act	magnetite (hm, cp)	P=0.6lkb,Tgar 550->700°C, NaCl 15-50 wt% Tgar 100-250°C, NaCl 0-25 wt% KCl>CaCl>NaCl daughters in mt, mt∂18O=2.0 cc∂18O=2.5-6.9, cc∂13C= -7.2-3.6	Lamey, 1948, 1961; Dubois and Brummett, 1968; Hall et al., 1988
Calcic Iron	Vancouver Island (Lake Iron Crown, Iron Hill, Paxton, Merry Widow) B.C., Canada	(Lake 27 Mt, ~50% Fe ~0.2% Cu	Oceanic island arc	Jurassic gabbro-diorite-granodiorite, extensive albite>cp>garnet endoskarn	Late Triassic basalt and limestone, Jurassic tuffs, breccia, and greenstone	gar(Ad15-98, Sp0-4, Sh0-7) > pyx(Hd10-95, Jo1-50, avg <3) epidote, ilvaite, hbd, act, chl	magnetite, (cp, py, po) > sl, cobaltite, asp, Au)	Tpyx 390-690°C, NaCl 3->26 wt% Tgar 370-460°C, NaCl 10-50 wt%, Tep 245-250°C NaCl and KCl daughter minerals	Sangster, 1969; Meinert, 1984; Bloomer, 1986; Ray and Webster, 1991b
Calcic Iron	Sarbai, Turgai Province West Siberia, USSR	725 mt, 45.6% Fe, 0.04% Cu, 0.05% Zn, 0.017% Pb	Oceanic island arc	Hercynian diorite bio, albite, scap	Carboniferous andesite, tuff, lmst argillite	garnet, pyroxene, magnetite	magnetite, (cp, py, cobaltite, asp, Au)		Sokolov and Grigorev, 1977
Gold	Nickel Plate Mine, Hedley District, British Columbia, Canada	3 Mt 14 g/t Au u.g.; 5.1 Mt 3 g/t Au o.p.; 1.4 g/t Ag; 0.03% Cu	accreted oceanic back arc basin	Jurassic porphyritic stock and dyke swarm biotite, kspar, plag (An24-52), act, ep, pyx, gar endoskarn	Upper Triassic siltstone, tuff, shale, limestone, conglomerate, andesite breccia	early bio-kspar hornfels pyx(Hd60-94, Jo1-4) >> gar(Ad14-82, avg 35, Sp<2) act, wo, scap, kspar, ep, preh	asp>po>>cp,py,sl>co hedleyite, native bismuth and gold> gl, maldonite, lo	Tpyx 250-695°C, avg 368°C Tgar 210-730°C, avg 384°C NaCl 5-33 wt% Tscap 320-400°C, avg 348°C	Ray et al, 1988; Ettlinger, 1990; Ray and Webster, 1991a; Ettlinger et al., 1992
Gold	Fortitude Mine, Copper Canyon District, Nevada, USA	11 Mt 5.3 g/t Au o.p. (5.1 Mt 10.5 g/t Au) <0.1% Cu	subduction beneath accreted, possibly oceanic crust (?)	38 Ma lim-bearing porphyritic stock & dyke kspar-biotite veins and dissem endoskarn	Penn.-Permian limestone, siltstone, conglomerate, shale	early bio-kspar hornfels pyx(Hd20-95, Jo1-10) >> gar(Ad40-97, avg 60, Sp<2) act, chl, prehnite	po>>py, sl, asp, mt, cp> hedleyite, native bismuth & gold	Tpyx 350-500°C*, avg NaCl 15 wt% qz veins in stock∂18O=11.3-15.1, ∂D=-102:-76 bio veins in stock∂18O=3.3-7.8, ∂D=-139:-100	Batchelder, 1977; Wotruba et al., 1988; Myers and Meinert, 1991; Theodore et al., 1991
Gold	Crown Jewel, Buckhorn District, Washington, USA	7.4 Mt 3.5 g/t Au o.p. <0.1% Cu	accreted oceanic back arc basin	Mesozoic (?) lim-bearing granodiorite stock and dykes bio, kspar, albite ep-gar-pyx endoskarn	Upper Paleozoic intercalated limestone, siltstone, conglomerate, andesite-basalt	early bio-pyx-amph hornfels gar(Ad18-99, avg 50, Sp<2) > pyx(Hd20-94, Jo1-4) ep>act, zoisite	magnetite>po>>py, mc cp, bismuthinite > cobaltite, native Au & bismuth, arsenopyrite	Tgar 465-550°C*, Tpar 355-470°C* NaCl 19-22 wt% Tep 305-420°C*, Tact 370-400°C*	Hickey, 1990
Tungsten	MacMillan Pass, Yukon-Northwest Territories, Canada	32 Mt 0.92% WO3	Continental collision/ subduction (?)	90 Ma granite kspar megacrysts myrmekite	Cambrian to Silurian intercalated limestone, shale, & siltstone	pyx(Hd45-94, Jo3-10) > gar(Ad2-10, Sp+Al 24-56) wo, ido, bio, hbd, clz, chl	scheelite > po, cp (py, mo, ferberite)	P 2.1-2.5kb, X(CH4>>N2>H2S>CO2) <0.04 Tgar = 350-440°C*, NaCl = 4.1-8.5 eq wt% Tpyx = 330-400°C*, NaCl = 2.5-9.2 wt% Tqtz = 320-470°C*, NaCl = 2.5-10.5 wt%	Dick and Hodgson, 1982; Atkinson and Baker, 1987; Gerstner et al., 1989
Tungsten	Pine Creek, California, USA	>6 Mt 0.5% WO3	Continental collision/ subduction (?)	92 Ma granite, pegmatitic pods myrmekite pyx-plag-ep-gar endoskarn	Upper Paleozoic shale, limestone, sandstone	gar(Ad20-72, Sp+Al 5-80) pyx(Hd50-82, Jo3-18) ido, wo, plag, hbd, bio, chl ep, fl, sp, sphene, zeolites	scheelite > cp, mo > mt, py, (po, sl)	P=1.5-2kb, XCO2=0.03-0.2, Tp 450-600°C, Tr 350-450°C gar∂18O=4.5-7.5, pyx∂18O=4.9-6.9, qz∂18O=5.6-10.7 cc∂18O=16.4-22, cc∂13C=-10.2:-3.6, ep∂D=-141 amph∂D=-146:-162, mo∂34S=4.5-5.8 cp∂34S=5.0-5.8, py∂34S=4.9-5.3, po∂34S=5.7	Newberry, 1982; Brown et al., 1985
Tungsten	King Island, Tasmania, Australia	14 Mt 0.8 WO3	Continental collision/ subduction (?)	345 Ma granodiorite - granite aplite & pegmatite dykes myrmekite pyx-plag endoskarn	Upper Proterozoic to Cambrian marl, siltst. conglomerate, basalt, dolostone, limestone	gar(Ad54-98, Sp 1-5) pyx(Hd23-98, Jo1-9) (ido, wo), ferrohastingsite ep, apatite	scheelite > py, mo > (cp, sl, gl) bismuthinite early scheelite contains up to 34% powellite	P = 0.65-1.3 kb, Tgar = 290-800°C, Total salinity = 23-65 wt% Tpyx = 350-600°C, Total salinity = 28-52 wt% Tsch = 270-520°C, Total salinity = 20-50 wt% Tamph = 250-380°C, Total salinity = 12-28 wt% Fl daughter minerals: NaCl, KCl, CaCl2, NaAlCO3(OH)2 FeCl2, Fe2O3, Fe3O4, local liquid CO2 in Fl, sch∂18O=3.5-5.7 gar∂18O=4.7-7.3, pyx∂18O=6.7-8.9, qz∂18O=3.5-11 mo∂34S=10.7-12.2, py∂34S=9.9-14.4, po∂34S=9.1-13	Kwak, 1978a,b; Tan and Kwak, 1979; Kwak and Tan, 1981; Wesolowski, 1984
Tungsten	Salau, Pyrénées, France	>1.1 Mt 1.54% WO3	Continental collision/ subduction (?)	Hercynian (270-290 Ma) granite-monzogranite stock pyx-plag endoskarn, ep, amph qz-muscovite-tourmaline	Silurian-Devonian interbedded graphitic limestone>shale, local sandstone and marl	pyx(Hd35-99, Jo2-10) >> gar(Ad5-20, Sp+Al 6-52) wo, ido, hbd, ferroactinolite biotite hornfels, clinozoisite	scheelite > po, cp, sl asp, (mo, bi, stannite) bismuthinite	P=2-2.6kb, X(CO2>CH4>>N2>H2S)=0.05-0.2 Tgar-pyx 455-570°C*, NaCl 23-30 eq. wt%, NaCl daughters Tsch 415-500°C*, amph∂18O=6.8, amph∂D=-80 cc∂18O=9.5-14.7, cc∂13C= -9.6:-3 po∂34S=6-2, cp∂34S=0.5-2.5, sl∂34S=2.5-4	Fonteilles et al., 1989

Skarn Type	Name & Location	Tonnage and Grade	Tectonic Setting	Pluton & Alteration	Protolith	Skarn Mineralogy	Ore Mineralogy	Geochemistry	References
Copper	Mines Gaspé, Quebec, Canada	skarn 62 Mt 1.25% Cu 0.03% Mo, u.g. porphyry 274 Mt, o.p. 0.4% Cu, 0.03% Mo	Continental subduction	Late Devonian qtz monzonite; secondary kspar-bio veins & disseminated, qtz-ser-py veins; kaolinite, calcite, anhydrite	Lower Devonian carbonaceous silty limestone, calcareous siltstone and shale	andraditic garnet; diopsidic to hedenbergitic pyx; ido, wo, trem, ph, scapolite; act, ep, chl	py, po, cp, bn, sl, sch; tennantite, tetrahedrite	P(Fl)=0.12-0.38kb, T skarn 334-506°C, NaCl15-56 eq wt% Tlate qtz 138-470°C, NaCl 4-47 eq wt%, local CO2(liq) NaCl>>KCl daughter minerals, cδ18O=7.4-14.5 cδ13C=-9.5:-5.6, qtzδD=-61:-42, pyδD=-51, slδD=-51 cpδ34S=-1.4:+1.2, poδ34S=-1.5-0, bnδ34S=-0.8	Allcock, 1982; Gilmour, 1982; Shelton and Rye, 1982; Shelton, 1983
Copper	Santa Rita, New Mexico, USA	>100 Mt 0.9% Cu o.p.	Shallow angle continental subduction	60 Ma granodiorite/qtz monzonite porphyry stocks; kspar-bio & qtz-ser-py veins	Pennsylvanian cherry limestone, calcareous shale and shale	gar(Ad60-100, avg. 95) > pyx(Hd5-30), wo, tr, act, bio; chl, montmorillonite, siderite	mt>py>>sl (cubanite, mo)	P(Fl)=0.12-0.52kb, Tgar 325->450°C, NaCl 14->26 eq wt% Tqz 200-530°C, NaCl 15-34 eq wt%, NaCl>KCl>Fe2O3 daughter minerals, qtz veins in stock δ18O=6.6-8.5	Nielsen, 1970; Sheppard et al., 1971; Ahmad and Rose, 1980
Copper	Carr Fort, Bingham District, Utah, USA	250 Mt 2% Cu+, u.g. 150 Mt 1.2% Cu, u.g. 0.03% Mo, 14 g/t Ag	Shallow angle continental subduction	38 Ma qtz monzonite porphyry stock, dykes, bx; potassic>sericite, ep, amph	Pennsylvanian quartzite, calcareous siltstone, interbedded limestone	gar(Ad60-100, avg. 98) > pyx(Hd5-35), wo, tr, act, bio; chl, nontronite, talc, opal	mt,py>cp>bn (sl,gl)	P=0.2-0.8kb, qtz veins in stockδ18O=9.1-9.4	Sheppard et al., 1971; Atkinson and Einaudi, 1978; Einaudi, 1982a,b
Zinc-Lead	Vetadeta District, Durango, Mexico	15 Mt 5% Zn, 4% Pb 2.5% Cu 175 g/t Ag 0.5 g/t Au	Shallow angle continental subduction (?)	33.1 qtz latite porphyry stock and dykes; secondary kspar, sericite; ep,chl, calcite endoskarn	Cretaceous massive gray limestone with local chert nodules	gar(Ad39-99, Sp0-3) >> wo; no pyroxene reported; ep, act, clz, zoisite	sl,gl>po>cp,asp,py; freibergite, boulangerite Tgar(tec.) 442-472°C; no hematite or magnetite reported	P = 0.73 kb (Fl), Tgar(prim.) 462-586°C, NaCl 8-13 eq wt% NaCl 32, KCl 24 wt% Tfl 324-403°C; NaCl 33, KCl 20 wt% poδ34S=0.2, aspδ34S=2, gδ34S=-1.4, slδ34S=-1:+1	Gilmer et al., 1988a; Gilmer et al., 1988b; Megaw et al., 1988
Zinc-Lead	Naica, Chihuahua, Mexico	21 Mt 3.8% Zn, 4.5% Pb, 0.4% Cu 150 g/t Ag, 0.3 g/t Au	Shallow angle continental subduction (?)	Tertiary (?) rhyolite dykes; garnet-idocrase endoskarn	Cretaceous homogeneous clean limestone, shale	gar(Ad20-98; Sp2-7) > pyx(Hd40, Jo40), ido, bust fluorite, chl, amphibole	sl,gl>py>cp,asp,po; mt (molybdenite)	P=0.3 kb, Tfl 120-680°C, NaCl 22-63, KCl 10-30 eq wt% CO2>CH4; NaCl>KCl>CaCl, cδ18O=7.5-16, cδ13C=-6.5:-1.2, gδ34S=2.9-4.4, slδ34S=3.8-5.7	Erwood et al., 1979; Megaw et al., 1988; Haynes and Kesler, 1988
Zinc-Lead	Groundhog Mine, Central District, New Mexico, USA	3 Mt 12.3% Zn 3.6% Pb, 1.3% Cu 86 g/t Ag	Shallow angle continental subduction	60 Ma granodiorite porphyry dykes with extensive ep>chl>(gar,pyx) endoskarn	Mississippian-Penn. limestone interbedded with black shale	pyx(Hd5-80, Jo5-85) >> gar(Ad35-98, avg. 92; Sp1-8) bust, ilvaite, chl, danneморite	sl>gl>py,cp,mt; hm (tetrahedrite)	P = 0.2 kb (Fl), Tpyx 230-425°C, NaCl 2->26 eq wt% Tgar 290-390°C, NaCl 2->26 eq wt%, Tsl 230-420°C temp & salinity zoned relative to dikes	Meinert, 1987
Zinc-Lead	Nakatasu Mine, Fuku Prefecture, Japan	7 Mt 5.5% Zn 0.5% Pb, 0.3% Cu 30 g/t Ag	volcanic arc subduction	early Tertiary (65 Ma) granite porphyry; ser-chl alteration, clinozoisite, ep, amph	Carboniferous black limestone and interbedded black slate	pyx(Hd21-98, Jo14-98) > gar(Ad16-99, Sp2-8), wo, ilv; ferroact, bust, fl, neotroцite	sl>gl>po,cp,py,mt> asp	Tasp 350-450°C, cδ18O=8.8-16.8, cδ13C=-7.5:-3.8 gδ34S=1.0-3.5, poδ34S=4.3, slδ34S=3.4-5.6	Shimizu and Iiyama, 1982; Shimizaki, 1988
Molybdenum	Azegour, Morocco	>0.13 Mt 1% MoS2 minor Cu, W, U	Transitional tectonism	Mesozoic granite	Paleozoic limestone, schist	gar, hd pyx, ido, amphibole	mo>cp, sl, py, pitchblende		Permingeat, 1957
Molybdenum/ Tungsten	Tyrnyauz, Republic of Georgia, USSR	>1 Mt Mo:W 4:1 to 1:8	Transitional tectonism	97 Ma granite porphyry; wo-pyx endoskarn, qtz-mo stockwork veins	Devonian-Lower Carboniferous shale, siltstone	pyx(Hd60-70) > gar(Ad30-94) plag, wo, ido, fl, apatite, act ep, ilvaite, xonotlite, sphene	mo, sch, powellite, cp, po, sl, asp, gl, mt bismuthinite, tellurides	Tfl 650-800°C; NaCl+KCl 60-70 total wt% daughter minerals: NaCl>KCl>Fe2O3, CaCO3 CaF2, graphite, asp, cp, sl: CO2, N2, CH4	Akmetov and Grekov, 1982; Goleva and Kulikov, 1988; Kulikov and Boyarskaya, 1989
Molybdenum	Little Boulder Creek, Montana, USA	167 Mt 0.15% MoS2	Transitional tectonism	Cretaceous quartz monzonite aplite, qtz veins with kspar	Pennsylvanian silty limestone, quartzite	pyx(Hd70,Jo3) > gar(Ad40) wo, scap, fluorite	mo, py, sch, cp, asp	P=0.45-1kb, Tep 410-500°C*, Total salinity = 1-34 wt%	Schmidt and Worthington, 1977, Cavanaugh, 1978
Tin	Mona, Tasmania, Australia	30 M: 0.15% Sn 0.05-0.1% W	Postorogenic rifting (?)	Devonian muscovite > biotite granite, pegmatite qtz-musc-fl-topaz greisen	Ordovician limestone sandstone	gar(Ad63-69; Sp4-6, Sn), tour pyx(Hd62,Jo1), Fe-amph, bio ep, ido, ep, sphene, topaz, fl	mt>cp>cassiterite> sch, cp, hematite, sl py, mo, bismuthinite	Tqtz 319-343°C, Total salinity 30-40 wt%, NaCl>KCl, CO2L Tfl 473-492°C, Total salinity 30-40 wt.%, NaCl>KCl>CaF2 poδ34S=8-6, pyδ34S=8.4-9.1, slδ34S=9.3	Kwak and Askins, 1981
Tin	Lost River, Alaska	3 Mt 0.27% Sn	Postorogenic rifting (?)	70 Ma biotite granite stock and rhyolite dykes with qtz-topaz-fl-tourmaline	Ordovician argillaceous limestone dolomite	gar(Ad15-95; Al+Sp5-42, Sn) pyx(Hd60,Jo3), bio, Fe-amph ep, ido, ep, fl, chl, helvie	mt>po>cassiterite> sch, cp, gl, sl, asp py, mo, bismuthinite	P(Fl) = 0.2-0.4 kb, Tfl 250-410°C, 6-28 wt% NaCl eq. xCO2<0.02, rare carbonate (?) > CaF2>NaCl daughter minerals	Dobson, 1982, 1984
Tin	JC, Yukon Territory, Canada	1.25 Mt 0.54% Sn	Postorogenic	100 Ma alkali-feldspar granite seriate to porphyritic with miarolitic cavities; fluorite, tourmaline, sericite greisen	Mississippian quartzite with thin marble layers	gar(Ad50-99; Sp≤2, Sn) > hedenbergitic pyx, Fe-amph, epidote, axinite, sphene, beryl, tourmaline, danalite, biotite, fluorite, chl, muscovite	py,mt>cassiterite> asp, cp, marcasite, sl py, native bismuth	P=0.45-1kb, Tep 410-500°C*, Total salinity = 1-34 wt% Tax 410-490°C, Total salinity = 25-27 wt%, Tca 430-570°C* Total salinity = 25-43 wt%, Fl CaCl2>>NaCl>KCl gar(Gr)δ18O=9.6-10.5, gar(Ad)δ18O=6.1-6.8 amphδD=0-2:7.5, amphδD=-183:-165, cpδ18O=6.7:-4.6 epδD=-142:-109, cεδ18O=-0.4-8.4, cεδ13C= -7.9:-4.1 poδ34S=0.1-0.6, cpδ34S=0.5-0.7, aspδ34S=0.4-2.7	Layne and Spooner, 1991; Layne et al., 1991

abbreviations: act = actinolite, Ad = andradite, Al = almandine, amph = amphibole, An = anorthite, ap = apatite, asp = arsenopyrite, ax = axinite, bio = biotite, bust = bustamite, bx = breccia, chl = chlorite, clz = clinozoisite, co = cobaltite
cp = chalcopyrite, cs = cassiterite, ep = epidote, Fl = fluid inclusion, fl = fluorite, gar = garnet, gl = galena, hbd = hornblende, Hd = hedenbergite, hm = hematite, ido = idocrase, Jo = johannsenite, lo = boulangerite, mc = marcasite, mt = magnetite
m.t. = million tons, o.p. = open pit mine, p.g = pegmatite, ph = phlogopite, plag = plagioclase, po = pyrrhotite, prch = prehnite, py = pyrite, pyx = pyroxene, qz = quartz, scap = scapolite, sch = scheelite, ser = sericite
serp = serpentine, sl = sphalerite, Sp = spessartine, T() = borno. T°C of Fl in indicated mineral; Tp(t) = T°C estimate from prograde (retrograde) mineral equilbria, trem = tremolite, u.g. = underground mine, wo = wollastonite, * = pressure corrected

sus sulphide-rich, and greisen *versus* skarn. Unfortunately, few of these categories are mutually exclusive. Like the zinc skarns, many large tin skarn systems are zoned from skarn rich to skarn poor (or absent). For example, in the Renison Bell area of Tasmania, there is a single large magmatic/hydrothermal system zoned from a proximal, calcic tin skarn, with minor cassiterite disseminated in a sulphide-poor garnet-pyroxene gangue, to a distal, magnesian massive sulphide replacement body, containing abundant cassiterite and a complete absence of calc-silicate minerals. The distal massive sulphide ore body (Renison Bell) is a major ore deposit and the proximal skarn body (Pine Hill) has not been and probably never will be mined. Einaudi *et al.* (1981) emphasized that there is a common thread linking the several types of tin skarn deposits: the characteristic suite of trace elements (Sn, F, B, Be, Li, W, Mo and Rb) in the ore and in associated igneous rocks. This suite distinguishes tin skarns from all other skarn types. Kwak (1987) makes a further distinction in that many tin skarn deposits develop a greisen alteration stage which is superimposed upon the intrusion, early skarn, and unaltered carbonate. Greisen alteration is characterized by high-fluorine activities and the presence of minerals like fluorite, topaz, tourmaline, muscovite, grunerite and ilmenite, and abundant quartz. In many cases, this greisen-stage alteration completely destroys earlier alteration stages. Of particular importance, greisen-style alteration is absent from all other skarn types. For a more thorough review of tin skarn systems and greisens, see Kwak (1987).

There are several mineralogical features of tin skarns that should be highlighted. From a mining standpoint, the most important is that tin can be incorporated into silicate minerals, such as garnet, titanite and vesuvianite, where it is economically unrecoverable. Dobson (1982) reports garnet containing up to 6% Sn in skarn at Lost River, Alaska. Thus, large deposits such as Moina in Tasmania (Kwak and Askins, 1981) can contain substantial amounts of tin that cannot be recovered with present or foreseeable technology. Extensive retrograde or greisen alteration of early tin-bearing skarn minerals can liberate this tin and cause it to precipitate in oxide or sulphide ore. Thus, the skarn destructive stages of alteration are particularly important in tin skarn deposits. As noted by Kwak (1987), the most attractive ore bodies occur in the distal portions of large skarn districts, where massive sulphide or oxide replacements occur without significant loss of tin in calc-silicate minerals like garnet.

Other Skarn Types

There are many other types of skarn which historically have been mined or explored for a variety of metals and industrial minerals. Some of the more interesting include rare

earth element (REE)-enriched skarns (*e.g.*, Guiliani *et al.*, 1979; Kato, 1989). REEs tend to be enriched in specific mineral phases such as garnet, vesuvianite, epidote and allanite. Vesuvianite and epidote with up to 20% REE (Ce>La>Pr>Nd) have been found in some gold skarns and zinc skarns (Gemmell *et al.*, 1992; Meinert, unpublished data). Some skarns contain economic concentrations of REEs and uranium (Kwak and Abeysinghe, 1987; Lentz, 1991). The Mary Kathleen skarn deposit in Queensland, Australia, is unusual in that REE and uranium daughter minerals in fluid inclusions suggest that these elements can be strongly concentrated in high-temperature hydrothermal fluids (Kwak and Abeysinghe, 1987). This suggests that other metasomatic environments should be examined for possible concentrations of REEs and uranium.

The occurrence of platinum group elements (PGE) is reported in some skarns (*e.g.*, Knopf, 1942). These deposits have not been well documented in the literature and most appear to represent metasomatism of ultramafic rocks (*e.g.*, Yu, 1985). It is difficult to evaluate the abundance of PGEs in different skarn types because PGEs have not been routinely analysed until recently. Geochemical considerations suggest that PGEs could be transported under very acidic, oxidized conditions (Wood *et al.*, 1989). In the skarn environment, such conditions might be reached in the greisen alteration stage of tin skarns. This might be a direction for future research and exploration.

Another skarn type that has received recent study is related to metasomatism in regional metamorphic environments (Mueller, 1988; Llotka and Nesbitt, 1989; Pan *et al.*, 1991). In the Yilgarn craton of Western Australia, Archean volcanic rocks are cut by regional shear zones which host gold-quartz veins with typical carbonate-sericite alteration in most deposits (Groves *et al.*, 1988). In some of the deeper deposits, mineralized gold-quartz veins have zoned alteration envelopes of calcic pyroxene and garnet (Mueller, 1988). Skarn alteration is locally massive and best developed in iron-rich metabasalt, banded iron formation, and komatiite. Based upon detailed underground mapping, mineral equilibria, and structural fabrics, Mueller (1988) interprets the skarn alteration as post-dating peak metamorphism and related to synkinematic granite domes.

In the Archean Slave Province of northern Canada, banded iron formation contains disseminated and vein-controlled gold mineralization associated with arsenopyrite and pyrite at the Lupin Mine. Metamorphism of these rocks has formed hedenbergitic pyroxene skarn along with grunerite and garnet. Llotka (1988) noted that hedenbergite skarn is most abundant in the central sheared part of the Lupin Mine, and concluded that metasomatic fluids circulating along the shear

zone were responsible for stabilizing the calcic hedenbergite pyroxene in the iron-rich, but calcium-poor, host rocks. However it formed, the arsenopyrite-bearing hedenbergite skarn at Lupin is very similar in composition and texture to some of the Phanerozoic gold skarns described in Table 2.

GEOCHEMISTRY AND GEOPHYSICS

Most geochemical studies of skarn deposits have focussed on mineral phase equilibria, fluid inclusions, isotopic investigations of fluid sources and pathways, and determination of exploration anomaly and background levels. Experimental phase equilibria studies are essential for understanding individual mineral reactions, such as the very simple ones illustrated in Figure 2. Such studies can be extended by using thermodynamic data to include variable compositions (*e.g.*, Bowman and Essene, 1982). Another approach is to use a self-consistent thermodynamic database to model potential skarn-forming solutions (*e.g.*, Flowers and Helgeson, 1983; Johnson and Norton, 1985; Ferry and Baumgartner, 1987). Fractionation of elements between minerals (*e.g.*, Ca:Mg in carbonate; Bowman and Essene, 1982) also can be used to estimate conditions of skarn formation.

Fluid inclusion studies of many ore deposit types focus on minerals, such as quartz, carbonate and fluorite, that contain numerous fluid inclusions, are relatively transparent, and are stable over a broad T-P-X range. This broad T-P-X range can, however, cause problems in interpretation of fluid inclusion data because these minerals may continue to grow and to trap fluids from early high-temperature events through late low-temperature events (Roedder, 1984). In contrast, high-temperature skarn minerals, such as forsterite and diopside, are unlikely to trap later low-temperature fluids (beyond the host mineral's stability range) without visible evidence of alteration. Thus, fluid inclusions in skarn minerals provide a relatively unambiguous opportunity to measure temperature, pressure and composition of skarn-forming fluids.

Much of the skarn fluid inclusion literature prior to the mid-1980s, especially studies of Sn and W skarn deposits, has been summarized by Kwak (1986). Such studies have been very useful in documenting the high temperatures (>700°C) and high salinities (>50 wt.% NaCl equivalent and multiple daughter minerals) which occur in many skarns. All the skarn types summarized in Table 2, except for copper and zinc skarns, have fluid inclusions that yield homogenization temperatures up to and exceeding 700°C. Homogenization temperatures in most fluid inclusions in copper and zinc skarn deposits are in the 300-550°C range. This is consistent with the relatively shallow and distal geologic settings inferred, respectively, for these two skarn types. Salinities in most skarn fluid inclusions are high; docu-
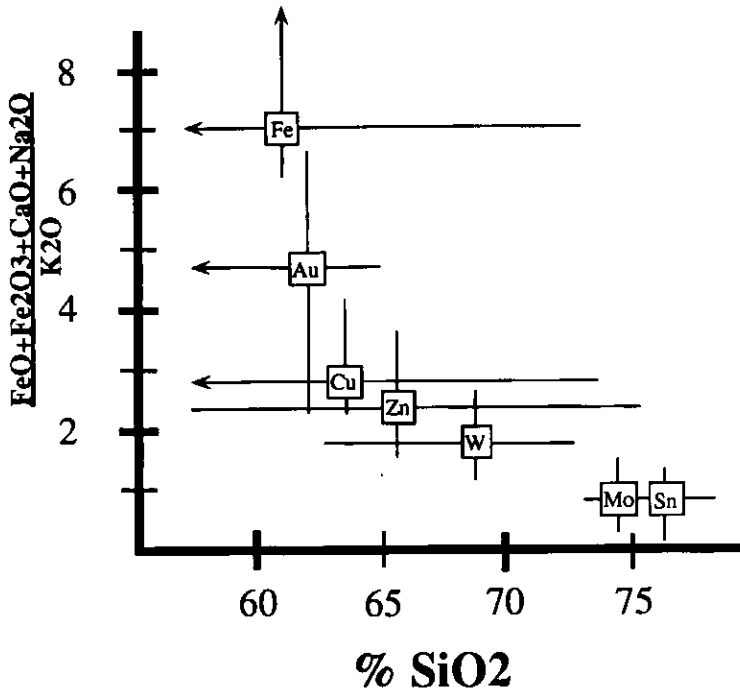
Figure 5 *Average composition of plutons associated with different skarn types. Modified from Meinert et al. (1990).*

mented daughter minerals in skarn minerals include NaCl, KCl, $CaCl_2$, $FeCl_2$, $CaCO_3$, CaF_2, C, $NaAlCO_3(OH)_2$, Fe_2O_3, Fe_3O_4, AsFeS, $CuFeS_2$ and ZnS (Table 2). Haynes and Kesler (1988) describe systematic variations in $NaCl:KCl:CaCl_2$ ratios in fluid inclusions from different skarns, reflecting differences in the fluid source and the degree of mixing of magmatic, connate and meteoric fluids. In general, magmatic fluids have $KCl>CaCl_2$, whereas high-$CaCl_2$ fluids appear to have interacted more with sedimentary wall rocks.

Fluid inclusions can provide direct evidence for the content of CO_2 (both liquid and gas), CH_4, N_2, H_2S and other gases in hydrothermal fluids. Studies of gas phases and immiscible liquids in fluid inclusions typically show a dominance of CO_2, a critical variable in skarn mineral stability. Although no comparative studies have been done, it appears that CH_4 is slightly more abundant than CO_2 in reduced systems like tungsten skarns (Fonteilles et al., 1989; Gerstner et al., 1989), whereas CO_2 is more abundant than CH_4 in more oxidized systems like copper and zinc skarns (Megaw et al., 1988).

Fluid inclusions in specific skarn mineral phases are particularly useful in documenting the temporal and spatial evolution of skarn-forming fluids, and how those changes correlate with compositional, experimental
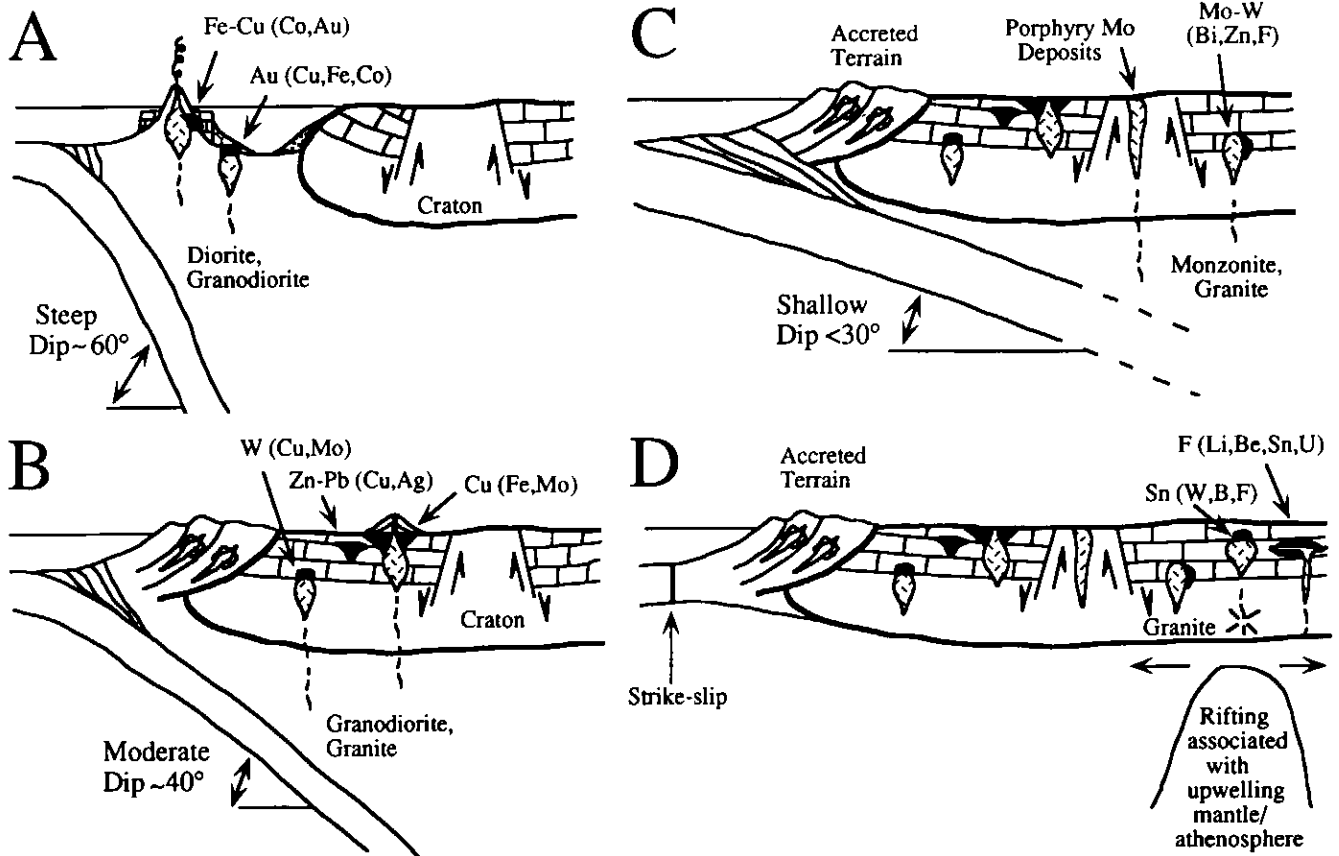

Figure 6 *Idealized tectonic models for skarn formation: (A) oceanic subduction and back arc basin environment; (B) continental subduction environment with accreted oceanic terrane; (C) transitional low-angle subduction environment, and (D) post-subduction or continental rifting environment (modified from Meinert, 1983).*

and thermodynamic data (*e.g.*, Kwak and Tan, 1981; Meinert, 1987). Fluid inclusions also provide direct evidence for the temperature and salinity shifts in most skarn systems between prograde and retrograde skarn events. For example, fluid inclusions in garnet and pyroxene in iron skarns have homogenization temperatures of 370->700°C and 300-690°C, respectively, with salinities up to 50 wt.% NaCl equivalent, whereas inclusions in retrograde epidote and crosscutting quartz veins have homogenization temperatures of 245-250°C and 100-250°C, respectively, with salinities of <25 wt.% NaCl equivalent (data from Table 2). In gold skarns, inclusions in prograde garnet and pyroxene have homogenization temperatures up to 730°C and 695°C, respectively, with salinities up to 33 wt.% NaCl equivalent. In contrast, inclusions in scapolite, epidote and actinolite from these skarns have homogenization temperatures of 320-400°C, 255-320°C, and 320-350°C, respectively. In tungsten skarns, inclusions in prograde garnet and pyroxene have homogenization temperatures up to 800°C and 600°C, respectively, with salinities up to 52 wt.% NaCl equivalent. In contrast, inclusions in amphibole and quartz from these skarns have homogenization temperatures of 250-380°C and 290-380°C, respectively, with salinities of 12-28 wt.% NaCl and 2.5-10.5 wt.% NaCl equivalent. Fluid inclusions in garnet and pyroxene from the MacMillan Pass tungsten deposit (Gerstner *et al.*, 1989) have homogenization temperatures and salinities that are anomalously low and at variance with most other studies of similar deposits, suggesting that further studies at MacMillan Pass might extend the range of presently available data.

Isotopic investigations, particularly the stable isotopes of C, O, H and S, have been critically important in documenting the multiple fluids involved in the formation of most large skarn systems (Shimazaki, 1988). The pioneering study of Taylor and O'Neill (1977) demonstrated the importance of both magmatic and meteoric waters in the evolution of the Osgood Mountain W skarns. Bowman *et al.* (1985) demonstrated that in high-temperature W skarns even some of the hydrous minerals, such as biotite and amphibole, can form at relatively high temperatures from water with a significant magmatic component (see also Marcke de Lummen, 1988). Specifically, garnet, pyroxene and associated quartz from the skarn deposits summarized in Table 2 all have $\delta^{18}O$ values in the +4 to +9‰ range, consistent with derivation from magmatic waters. In contrast, $\delta^{18}O$ values for sedimentary calcite, quartz and meteoric waters in these deposits are distinctly different. In most cases, there is a continuous mixing line between original sedimentary $\delta^{18}O$ values and calculated $\delta^{18}O$ values for magmatic hydrothermal fluids at the temperatures of prograde skarn formation. Simi-

lar mixing is indicated by $\delta^{13}C$ values in calcite, ranging from typical sedimentary $\delta^{13}C$ values in limestone away from skarn to typical magmatic values in calcite interstitial to prograde garnet and pyroxene (Brown *et al.*, 1985). Hydrous minerals such as biotite, amphibole and epidote from different skarn deposits also display $\delta^{18}O$ and δD values ranging from magmatic to local sedimentary rocks and meteoric waters (Layne *et al.*, 1991). Again, mixing of multiple fluid sources is indicated.

Sulphur isotopic studies on a variety of sulphide minerals (including pyrite, pyrrhotite, molybdenite, chalcopyrite, sphalerite, bornite, arsenopyrite and galena) from the skarn deposits summarized in Table 2, indicate a very narrow range of $\delta^{34}S$ values,

consistent with precipitation from magmatic fluids. For some of the more distal zinc skarns, sulphur isotopic studies indicate that the mineralizing fluids acquired some of their sulphur from sedimentary rocks (including evaporites) along the fluid flow path (Megaw *et al.*, 1988). Overall, stable isotopic investigations are consistent with fluid inclusion and mineral equilibria studies which demonstrate that most large skarn deposits formed from diverse fluids, including early, high-temperature, highly saline brines directly related to crystallizing magma systems (*e.g.*, Auwera and Andre, 1988). In many systems, the highest-salinity fluids are coincident with peak sulphide deposition. In addition, at least partial mixing with exchanged connate or meteoric fluids is required for most depos-
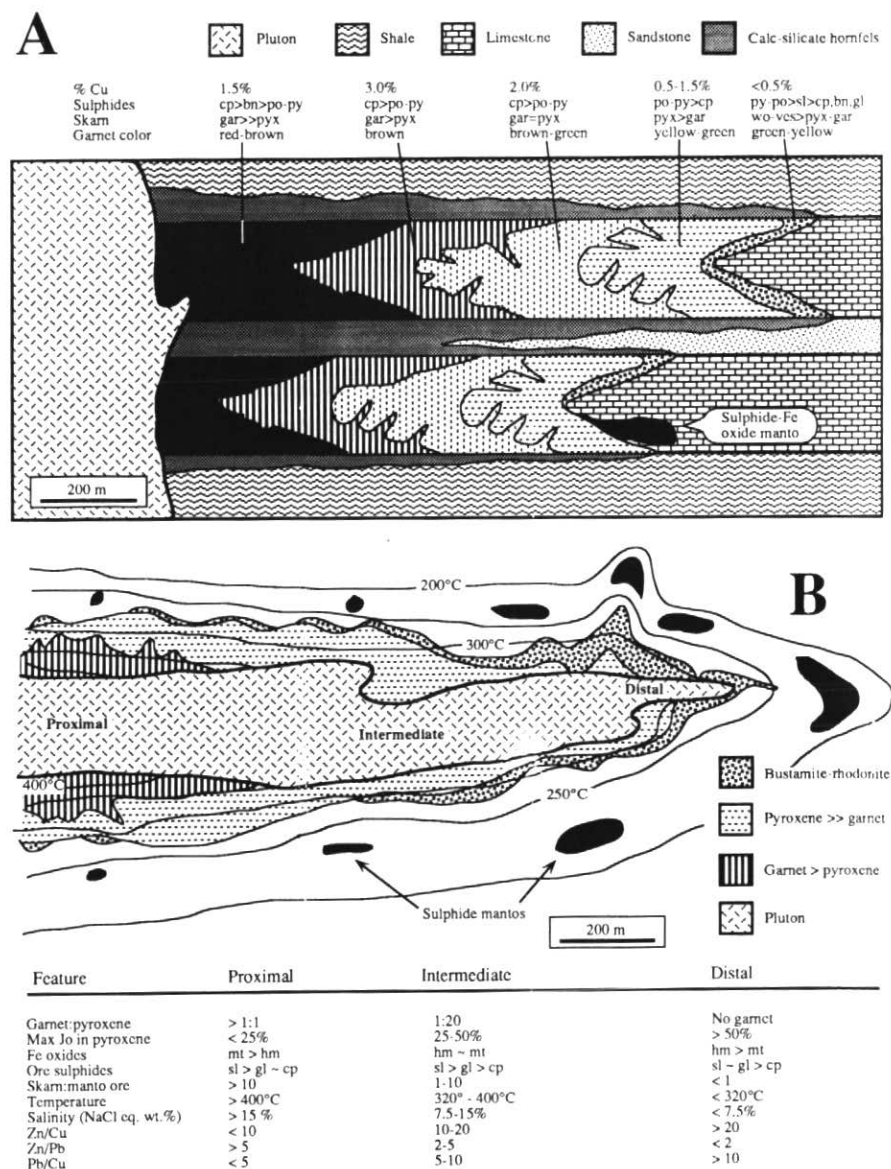
Figure 7 *General models of skarn zonation:* (A) *copper skarns (after Atkinson and Einaudi, 1978);* (B) *zinc skarns (after Meinert, 1987);* **(facing page)** (C) *gold skarns — Hedley District, British Columbia (after Ray and Webster, 1991a), and* (D) *gold skarns — cross section of the Fortitude deposit, Nevada (Myers and Meinert, 1991).*

its, with the latest alteration events forming largely from dilute meteoric waters.

Even though skarn metal contents are quite variable, anomalous concentrations of pathfinder elements in distal skarn zones can be an important exploration guide. Geochemical studies of individual deposits have shown that metal dispersion halos can be zoned from proximal Cu-Mo-Fe assemblages to distal precious metal zones and Pb-Zn-Ag veins (e.g., Theodore and Blake,

1975). Anomalies of tens to hundreds of ppm for individual metals can extend for more than 1000 m beyond proximal skarn zones. Comparison of geochemical signatures among different skarn classes suggests that each has a characteristic suite of anomalous elements; background levels for a particular element in one skarn type may be highly anomalous in others. For example, Au, Te, Bi and As contents of 1, 10, 100 and 500 ppm, respectively, are not unusual for rocks and

soils at gold skarn properties, but are rare to absent for other skarn types (e.g., Meinert et al., 1990; Myers and Meinert, 1991).

Some skarns have a strong geophysical response (Chapman and Thompson, 1984; Emerson, 1986). Almost all skarns are significantly denser than the surrounding rock, and therefore may form a gravitational anomaly or seismic discontinuity. This is particularly evident in some of the large iron skarns, which may contain more than a billion tons of magnetite (specific gravity = 5.18). In addition, both skarns and associated plutons may form magnetic anomalies (Spector, 1972). Relatively oxidized plutons typically contain enough primary magnetite to form a magnetic high, whereas reduced plutons typically contain ilmenite, rather than magnetite, and may form a magnetic low (Ishihara, 1977). Skarns may form a magnetic high due to large concentrations of magnetite (e.g., Chapman et al., 1986) or other magnetic minerals such as high-temperature pyrrhotite (e.g., Wotruba et al., 1988). Since metasomatism of dolomitic rocks tends to form abundant magnetite, in magnesian skarn deposits it may be possible to distinguish original protolith, as well as the presence of skarn, from a strong magnetic anomaly (Hallof and Winniski, 1971; Chermeninov, 1988).

Disseminated and massive sulphide minerals may give strong IP, EM or magnetotelluric responses in skarn (Emerson and Welsh, 1988). However, electrical surveys of skarns need to be interpreted carefully because metasomatism of carbonate rock necessarily involves the redistribution of carbon. The presence of carbonaceous matter, especially if in the form of graphite, can strongly effect electrical surveys. Such carbon-induced anomalies may be distant from, or unrelated to, skarn ore bodies.

A few skarns contain sufficient uranium and thorium to be detectable by airborne or ground radiometric surveys (e.g., Mary Kathleen in Australia; Kwak and Abeysinghe, 1987). Detailed studies of such deposits demonstrate that relatively small skarns can be detected, and that different types of skarns can be distinguished (e.g., Lentz, 1991).

PETROGENESIS AND TECTONIC SETTING

Most major skarn deposits are directly related to igneous activity, and broad correlations between igneous composition and skarn type have been described by several workers (Zharikov, 1970; Shimazaki, 1980; Einaudi et al., 1981; Kwak and White, 1982; Meinert, 1983; Newberry and Swanson, 1986; Newberry, 1987; Newberry et al., 1990). Averages of large amounts of data for each skarn type can be summarized on a variety of compositional diagrams (e.g., Fig. 5) to show distinctions among skarn classes. Tin and molydenum skarns are typically associated
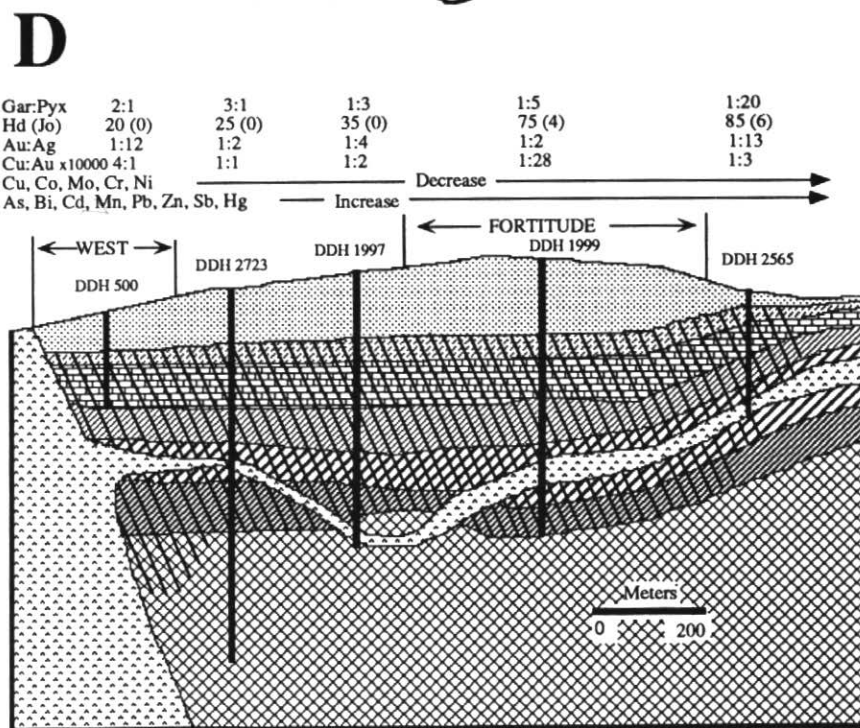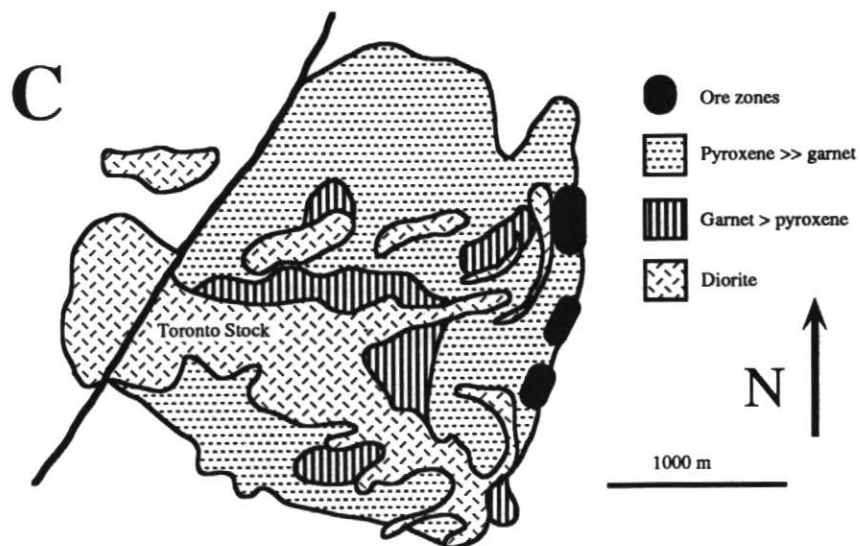
with high-silica, strongly differentiated plutons. At the other end of the spectrum, iron skarns are usually associated with low-silica, iron-rich, relatively primitive plutons. Such diagrams are less useful for detailed studies, however, because of the wide range of igneous compositions possible for an individual skarn deposit and the difficulty of isolating the effects of metasomatism and late alteration. Other important characteristics include the oxidation state, size, texture, depth of emplacement, and tectonic setting of individual plutons. For example, tin skarns are almost exclusively associated with reduced, ilmenite-series plutons which can be characterized as S-type or anorogenic. These plutons tend to form in stable cratons in which partial melting of crustal material may be instigated by incipient rifting. Many gold skarns are also associated with reduced, ilmenite-series plutons. Gold skarn plutons, however, are typically mafic, low-silica bodies which could not have formed by melting of sedimentary crustal material. In contrast, plutons associated with copper skarns, particularly porphyry copper deposits, are strongly oxidized, magnetite-bearing, I-type and associated with subduction-related magmatic arcs. These plutons tend to be porphyritic and emplaced at shallow levels in the earth's crust. Tungsten skarns, on the other hand, are associated with relatively large, coarse-grained, equigranular plutons or batholithic complexes indicative of a deeper environment.

Tectonic setting, petrogenesis and skarn deposits are intimately intertwined. Some modern textbooks use tectonic setting to classify igneous provinces (Wilson, 1989) or different kinds of ore deposits (Sawkins, 1984). This approach has been less successful in describing ore deposits, such as skarns, which are the result of processes that can occur in almost any tectonic setting. A useful tectonic classification of skarn deposits should group skarn types which are frequently found together, and distinguish those which are typical of specialized tectonic settings. For example, calcic Fe-Cu skarn deposits are virtually the only skarn type found in oceanic island-arc terranes (Fig. 6A). Many of these skarns are also enriched in Co, Ni, Cr and Au. In addition, some economic gold skarns appear to have formed in back-arc basins associated with oceanic volcanic arcs (Ray et al., 1988). Some of the key features that set these skarns apart from those associated with more evolved magmas and crust are their association with gabbroic and dioritic plutons, abundant endoskarn, widespread sodium metasomatism, and the absence of Sn and Pb. Collectively, these features reflect the primitive, oceanic nature of the crust, wall rocks, and plutons.

The vast majority of skarn deposits are associated with magmatic arcs related to subduction beneath continental crust (Fig.

6B). Plutons range in composition from diorite to granite, although differences among the main base metal skarn types appear to reflect the local geologic environment (depth of formation, structural and fluid pathways) more than fundamental differences of petrogenesis (Nakano et al., 1990). In contrast, gold skarns in this environment are associated with particularly reduced plutons that may represent a restricted petrologic history.

The transition from subduction beneath stable continental crust to post-subduction tectonics is not well understood. Magmatism associated with shallow subduction angles may have more crustal interaction (Takahashi et al., 1980), and floundering of the downward moving slab may result in local rifting. During this stage the magmatic arc may widen or migrate further inland. Plutons are granitic in composition, and associated skarns are rich in Mo or W-Mo, with lesser Zn, Bi, Cu and F (Fig. 6C). Many of these skarns are best described as polymetallic, with locally important Au and As.

Some skarns are not associated with subduction-related magmatism. These skarns may be associated with S-type magmatism, following a major period of subduction, or they may be associated with rifting of previously stable cratons. Plutons are granitic in composition, and commonly contain primary muscovite and biotite, dark gray quartz megacrysts, miarolitic cavities, greisen-type alteration, and anomalous radioactivity. Associated skarns are rich in tin or fluorine, although a host of other elements is usually present and may be of economic importance (Fig. 6D). This evolved suite includes W, Be, B, Li, Bi, Zn, Pb, U, F and REE.

MODELS AND CONCLUSIONS

Whether one thinks of skarn as a rock type or as an alteration of previously existing rocks, skarns are mappable in the field, and the basic map unit is defined by skarn mineralogy. A detailed map showing the distribution of skarn mineral phases will yield important information about the overall size, characteristics and genesis of a skarn system. Of course, the skarn mineralogy needs to be interpreted in terms of lithology, structure and timing. A given mineral may develop under different P-T-Xco_2 conditions in limestone relative to shale, or where fluid flow is enhanced by faulting or brecciation. Comparison of the field characteristics of a given occurrence with the general skarn features outlined in this paper provides a predictive basis for evaluating economic potential and overall genesis. Models of skarn zonation are particularly useful in evaluating incompletely exposed or explored skarn systems. Figure 7 presents general models for copper, zinc and gold skarns which combine skarn and ore mineralogy, metal ratios, and geochemical data. For particularly complex systems, such as tin skarns, a time-evolution model is useful for concurrent alteration in

igneous and sedimentary rocks (e.g., Dobson, 1982, fig. 8).

Skarns are one of the more variable classes of ore deposits, and the references cited in this paper and the more detailed review by Einaudi et al. (1981) will lead the reader to many variations upon the general theme. The purpose of the present paper has been to develop the general theme that skarn deposits are understandable, that they are amenable to mapping and simple field observations, and that modern geochemical techniques yield a fairly clear picture of their evolution. Skarns are distinct from many other types of ore deposits. Almost all large skarn deposits are directly related to igneous rocks. One of the fundamental controls of skarn mineralogy and metal content is the genesis and crystallization history of the associated pluton. The late-stage hydrothermal evolution of the pluton is mirrored by alteration and mineralization in the surrounding rocks. The reactivity of sedimentary rocks, particularly carbonate rocks, accounts for the abundance of skarns in most localities where magma is emplaced in the upper crust.

All skarn deposits form over a wide temperature range, but it is the high-temperature part of that range (>350°C) that distinguishes skarns from other ore types, such as Mississippi Valley-type Pb-Zn deposits, which may contain similar metals and form in similar rocks. The high temperatures and concentrated metasomatic fluids stabilize a variety of skarn minerals, such as garnet and pyroxene, which are the defining characteristic of skarns. The waning stages of hydrothermal activity invariably are cooler, and result in retrograde alteration of the early skarn minerals. This pattern of early metamorphism, followed by prograde and retrograde metasomatism, is common to most skarns. Variations on this general pattern are many, and include depth of formation, oxidation state, petrochemistry and wall rock composition.

In the world of economic geology, where fluctuating commodity prices and world demand can change an obscure skarn occurrence into a producing mine (and vice versa) in a short period of time, skarn deposits remain interesting economic and academic challenges. It is likely that skarn deposits will remain an important source of many metals in the next century. The challenge will be to predict which ones will be mined, and for what commodities.

ACKNOWLEDGEMENTS

past and present, are the sounding board for many of the ideas presented here. Dennis Beaver, Gail Bloomer, Jeff Brooks, Art Ettlinger, Mark Hawksworth, Bob Hickey, Greg Myers, Bill Neal, Dean Peterson, John Read and Kurt Wilkie deserve special mention. Finally, I would like to thank Pat Sheahan for her continuing encouragement.

REFERENCES

Agrell, S.O. and Charnely, N.F., 1987, Phosphoran olivines and phosphates of pallasitic affinities in skarns from Pine Canyon, Piute County, Utah, U.S.A.: Meteoritics, v. 22, p. 314-315.

Ahmad, S.N. and Rose, A.W., 1980, Fluid inclusions in porphyry and skarn ore at Santa Rita, New Mexico: Economic Geology, v. 75, p. 229-250.

Aksametov, E.V. and Grekov, I.I., 1982, Tirniauz tungsten-molybdenum ore deposits, in Tvalchrelidze, G.A., ed., Ore deposits of the Caucasus, Excursion A-1 and A-2 Guidebook: Metsniereba Publishing House, Tbilisi, USSR, p. 104-110.

Aksyuk, A.M. and Zharikov, V.A., 1988, The phlogopite skarn deposits: physical-chemical conditions of formation, in Zachrisson, E., ed., Proceedings of the 7th Quadrennial IAGOD Symposium: E. Schweizerbart'sche Verlagsbuchhandlung, Stuttgart, p. 321-326.

Allcock, J.B., 1982, Skarn and porphyry copper mineralization at Mines Gaspé, Murdochville, Quebec: Economic Geology, v. 77, p. 971-999.

Anovitz, L.M. and Essene, E.J., 1990, Thermobarometry and pressure-temperature paths in the Grenville Province of Ontario: Journal of Petrology, v. 31, p. 197-241.

Atkinson, D. and Baker, D.J., 1987, Recent developments in the geolgic understanding of MacTung, in Morin, J.A., ed., Mineral deposits of Northern Cordillera: Canadian Institute of Mining and Metallurgy, Special Volume 37, p. 234-244.

Atkinson, W.W., Jr. and Einaudi, M.T., 1978, Skarn formation and mineralization in the Contact Aureole at Carr Fork, Bingham, Utah: Economic Geology, v. 73, p. 1326-1365.

Auwera, J.V. and Andre, L., 1988, O, C and Sr isotopes as tracers of metasomatic fluids; application to the skarn deposit (Fe, Cu, W) of Traversella (Ivrea, Italy): Chemical Geology, v. 70, p. 137.

Barrell, J., 1907, Geology of the Marysville mining district, Montana: United States Geological Survey, Professional Paper 57, 178 p.

Barton, M.D., Staude, J-M., Snow, E.A. and Johnson, D.A., 1991, Aureole systematics, in Kerrick, D.M., ed., Contact Metamorphism: Mineralogical Society of America, Reviews in Mineralogy, v. 26, p. 723-847.

Batchelder, J., 1977, Light stable isotope and fluid inclusion study of the porphyry copper deposit at Copper Canyon, Nevada: Economic Geology, v. 72, p. 60-70.

Benkerrou, C. and Fonteilles, M., 1989, Vanadian garnets in calcareous metapelites and skarns at Coat an Noz, Belle Isle en Terre (Cotes du Nord), France: American Mineralogist, v. 74, p. 852-858.

Billingsley, P. and Hume, C.B., 1941, The ore deposits of Nickel Plate Mountain, Hedley, B.C.: Canadian Institute of Mining and Metallurgy, Bulletin, v. 44, p. 524-590.

Bird, D.K., Schiffman, P., Elders, W.A., Williams, A.E. and McDowell, S.D., 1984, Calc-silicate mineralization in active geothermal systems: Economic Geology, v. 79, p. 671-695.

Blackwell, D.D., Steele, J.L., Frohme, C.F., Murphey, C.F., Priest, G.R. and Black, G.L., 1990, Heat flow in the Oregon Cascade Range and its correlation with regional gravity, Curie Point depths, and geology: Journal of Geophysical Research, v. 95-B12, p. 19475-19493.

Bloomer, G.E., 1986, Geology, mineralogy, and geochemistry of the Iron Crown calcic iron skarn deposit, Vancouver Island, British Columbia: unpublished M.S. thesis, Washington State University, 115 p.

Bowers, J.R., Kerrick, D.M. and Furlong, K.P., 1990, Conduction model for the thermal evolution of the Cupsuptic aureole, Maine: American Journal of Science, v. 290, p. 644-665.

Bowman, J.R. and Essene, E.J., 1982, P-T-XCO$_2$ conditions of contact metamorphism in the Black Butte aureole, Elkhorn, Montana: American Journal of Science, v. 282, p. 311-340.

Bowman, J.R., Covert, J.J., Clark, A.H. and Mathieson, G.A., 1985, The CanTung E-zone scheelite skarn ore body, Tungsten, Northwest Territories: oxygen, hydrogen, and carbon isotope studies: Economic Geology, v. 80, p. 1872-1895.

Brooks, J.W., Meinert, L.D., Kuyper, B.A. and Lane, M.L., 1991, Petrology and geochemistry of the McCoy gold skarn, Lander County, NV, in Raines, G.L., Lisle, R.E., Schafer, R.W. and Wilkinson, W.H., eds., Geology and Ore Deposits of the Great Basin: Geological Society of Nevada, Reno, v. 1, p. 419-442.

Brown, P.E., Bowman, J.R. and Kelly, W.C., 1985, Petrologic and stable isotope constraints on the source and evolution of skarn forming fluids at Pine Creek, California: Economic Geology, v. 80, p. 72-95.

Burt, D.M., 1972, Mineralogy and geochemistry of Ca-Fe-Si skarn deposits: unpublished Ph.D. thesis, Harvard University, 256 p.

Burt, D.M., 1977, Mineralogy and petrology of skarn deposits: Society Italiana Mineralogia Petrolgia Rendiconti, v. 33, p. 859-873.

Burt, D.M., 1982, Skarn deposits — Historical bibliography through 1970: Economic Geology, v. 77, p. 755-763.

Caffrey, G.M., 1982, Petrology and alteration of ultramafic rocks of Bullrun Mountain, Baker County, Oregon: unpublished M.Sc. thesis, Washington State University, 130 p.

Cavanaugh, P.C., 1978, Geology of the Little Boulder Creek molybdenum deposit, Custer County, Idaho: unpublished M.Sc. thesis, University of Montana, 82 p.

Cavarretta, G., Gianelli, G. and Puxeddu, M., 1982, Formation of authigenic minerals and their use as indicators of physiochemical parameters of the fluid in the Larderello-Travale geothermal field: Economic Geology, v. 77, p. 1071-1084.

Cavarretta, G. and Puxeddu, M., 1990, Schorl-dravite-ferridravite tourmalines deposited by hydrothermal magmatic fluids during early evolution of the Larderello geothermal field, Italy: Economic Geology, v. 85, p. 1236-1251.

Chapman, B.H. and Thompson, D.T., 1984, Applications of geophysical logging within skarn-type deposits: The Log Analyst, v. 25, pt. 2, p. 13-24.

Chapman, R.H., Joseph, S.E. and Campbell, L.G., 1986, Magnetic exploration for skarn deposits, Ivanpah mining district, San Bernardino County, California: California Geology, v. 39, pt. 8, p. 171-178.

Chermeninov, V.B., 1988, Mapping of hydrothermally altered rocks according to a borehole section: Soviet Geology and Geophysics, v. 29, p. 88-97.

Cotta, B. von, 1864, Erzlagerstätten im Banat und in Serbien: Vienna, Ed. W. Braunmuller, 105 p.

Darling, R.S., 1990, Wide range of molybdenite stability reflected in vein assemblages at the carbonate-hosted Cannivan Gulch stockwork molybdenum deposit, southwest Montana: Geological Society of America, Abstract with Programs, v. 67, p. A180.

Dick, L.A. and Hodgson, C.J., 1982, The MacTung W-Cu (Zn) contact metasomatic and related deposits of the northeastern Canadian Cordillera: Economic Geology, v. 77, p. 845-867.

Dobson, D.C., 1982, Geology and alteration of the Lost River Tin-Tungsten-Fluorine deposit, Alaska: Economic Geology, v. 77, p. 1033-1052.

Dobson, D.C., 1984, Geology and geochemical evolution of the Lost River, Alaska, tin deposit: unpublished Ph.D. thesis, Stanford University, 200 p.

Dubois, R.L. and Brummett, R.W., 1968, Geology of the Eagle Mountain mine area, in J.D. Ridge, ed., Ore deposits of the United States, 1933-1967 (Graton Sales volume): American Institute of Mining, Metallurgy and Petroleum Engineers, New York, p. 1592-1606.

Einaudi, M.T., 1982a, Descriptions of skarns associated with porphyry copper plutons, southwestern North America, in Titley, S.R., ed., Advances in Geology of the Porphyry Copper Deposits, Southwestern North America: University of Arizona Press, p. 139-184.

Einaudi, M.T., 1982b, General features and origin of skarns associated with porphyry copper plutons, southwestern North America, in Titley, S.R., ed., Advances in Geology of the Porphyry Copper Deposits, Southwestern North America: University of Arizona Press, p. 185-210.

Einaudi, M.T., Meinert, L.D. and Newberry, R.J., 1981, Skarn deposits: Economic Geology, 75th Anniversary Volume, p. 317-391.

Emerson, D.W., 1986, Physical properties of skarns: Exploration Geophysics, v. 17, pt. 4, p. 201-212.

Emerson, D.W. and Welsh, H.K., 1988, Low-frequency permittivities of skarns and associated rocks: Geophysics, v. 53, p. 1233-1240.

Erwood, R.J., Kesler, S.E. and Cloke, P.L., 1979, Compositionally distinct, saline hydrothermal solutions, Naica mine, Chihuahua, Mexico: Economic Geology, v. 74, p. 95-108.

Ettlinger, A.D., 1990, A geological analysis of gold skarns and precious metal enriched iron and copper skarns in British Columbia, Canada: unpublished Ph.D. thesis, Washington State University, 246 p.

Ettlinger, A.D. and Meinert, L.D., 1991, Gold in the Soviet Union: A study of the Veselyi Mine, Siniukhinskoe District, Siberia, USSR: Economic Geology, v. 86, p. 185-194.

Ettlinger, A.D., Meinert, L.D. and Ray, G.E., 1992, Gold skarn mineralization and evolution fluid in the Nickel Plate Deposit, Hedley District–British Columbia: Economic Geology, v. 87, p. 1541-1565.

Ferry, J.M. and Baumgartner, L., 1987, Thermodynamic models of molecular fluids at the elevated pressures and temperatures of crustal metamorphism, in Carmichael, I.S.E. and Eugster, H.P., eds., Thermodynamic modeling of geological materials: minerals, fluids and melts: Reviews in Mineralogy, v. 17, p. 323-365.

Flowers, G.C. and Helgeson, H.C., 1983, Equilibrium and mass transfer during progressive metamorphism of siliceous dolomites: American Journal of Science, v. 283, p. 230-286.

Fonteilles, M., Soler, P., Demange, M., Derre, C., Krier-Schellen. A.D., Verkaeren, J., Guy, B. and Zahm, A., 1989, The scheelite skarn deposit of Salau (Ariege, French Pyrenées): Economic Geology, v. 84, p. 1172-1209.

Geijer, P. and Magnusson, N.H., 1952, The iron ores of Sweden: 19th International Geological Congress, Algiers 1952, v. 2, p. 477-499.

Gemmell, J.B., Zantop, H. and Meinert, L.D., 1992, Genesis of the Aguilar zinc-lead-silver deposit, Argentina: Contact metasomatic versus sedimentary exhalative: Economic Geology, v. 87, p. 2085-2112.

Gerstner, M.R., Bowman, J.R. and Pasteris, J.D., 1989, Skarn formation at the MacMillan Pass tungsten deposit (MacTung), Yukon and Northwest Territories. I. P-T-X-V characterization of the methane-bearing, skarn-forming fluids: Canadian Mineralogist, v. 27, p. 545-564.

Giere, R., 1986, Zirconolite, allanite and hoegbomite in a marble skarn from the Bergell contact aureole; implications for mobility of Ti, Zr and REE: Contributions to Mineralogy and Petrology, v. 93, p. 459-470.

Gilmer, A.L., Clark, K.F.J., Hernandez C.I., Conde, C. and Figueroa, S.J.I., 1988, Geological and mineralogical summary of the metalliferous deposits in the Santa Maria Dome, Velardeña, Durango, in Clark, K.F., Megaw, P.K.M. and Ruiz, J., eds., Lead-zinc-silver carbonate hosted deposits of northern Mexico: University of Texas-El Paso, Society of Economic Geologists Guidebook, p. 143-153.

Gilmer, A.L., Clark, K.F., Conde, C.J., Hernandez, C.I., Figueroa, S.J.I. and Porter, E.W., 1988, Sierra de Santa Maria, Velardeña Mining District, Durango, Mexico: Economic Geology, v. 83, p. 1802-1829.

Gilmour, P., 1982, Grades and tonnages of porphyry copper deposits. in Titley, S.R., ed., Advances in Geology of the Porphyry Copper Deposits, Southwestern North America: University of Arizona Press, p. 7-36.

Giuliani, G., Cheilletz, A. and Mechiche, M., 1987, Behaviour of REE during thermal metamorphism and hydrothermal infiltration associated with skarn and vein-type tungsten ore bodies in central Morocco: Chemical Geology, v. 64, p. 279-294.

Goldschmidt, V.M., 1911, Die kontakmetamorphose im Kristianiagebiet: Oslo Vidensk. Skr., I., Mat.-Natur, v. K1., no. 1, 483 p.

Goleva, G.A. and Kulikov, I.V., 1988, The problem of the skarn mineralization of the Caucasus: International Geology Review, v. 30, p. 676-683.

Greenwood, J.H., 1967, Wollastonite: Stability in H_2O-CO_2 mixtures and occurrence in a contact metamorphic aureole near Salmo, British Columbia: American Mineralogist, v. 52, p. 1669-1680.

Grigoryev, N.A., Sazonov, V.N, Murzin, V.V. and Gladkovskiy, 1990, Sulfides as gold carriers in skarn magnetite deposit skarns and ores: Geochemical International, v. 27, p. 142-146.

Groves, D.I., Ho, S.E., McNaughton, N.J., Mueller, A.G., Perring, C.S., Rock, N.M.S. and Skwarnecki, M.S., 1988, Genetic models for Archaean lode-gold deposits in Western Australia: Analogues of Phanerozoic Skarn Deposits, in Ho, S.E., and Groves, D.I., eds., Advances in Understanding Precambrian Gold Deposits, Vol. 2: Geology Department and University Extension, University of Western Australia, Publication 12, p. 1-22.

Guy, B., Faure, N., Le Loc, H.G. and Varenne, J.L., 1988, Etude microthermométrique des inclusions fluides des skarns a tungstene de Costabonne (Pyrenees, France): Comptes Rendus de l'Académie des Sciences, Série 2, Mécanique, Physique, Chimie, Sciences de l'Univers, Sciences de la Terre, v. 307, pt. 1, p. 33-38.

Hall, D.L., Cohen, L.H. and Schiffman, P., 1988, Hydrothermal alteration associated with the Iron Hat iron skarn deposit, eastern Mojave Desert, San Bernardino County, California: Economic Geology, v. 83, p. 568-587.

Hallof, P.G., and Winniski, E., 1971, A geophysical case history of the Lakeshore ore body: Geophysics, v. 36, p. 1232-1249.

Hames, W.E., Tracy, R.J. and Bodnar, R.J., 1989, Postmetamorphic unroofing history deduced from petrology, fluid inclusions, thermochronometry, and thermal modeling; an example from southwestern New England with Suppl. Data 89-13: Geology, v. 17, p. 727-730.

Harris, N.B. and Einaudi, M.T., 1982, Skarn deposits in the Yerington District, Nevada: Metasomatic skarn evolution near Ludwig: Economic Geology, v. 77, p. 877-898.

Haynes, F.M. and Kesler, S.E., 1988, Compositions and sources of mineralizing fluid for chimney and manto limestone-replacement ores in Mexico: Economic Geology, v. 83, p. 1985-1992.

Hernon, R.M. and Jones, W.R., 1968, Ore deposits of the Central Mining District, New Mexico, in Ridge, J.D., ed., Ore deposits of the United States, 1933-1967 (Graton Sales volume): New York, American Institute of Mining, Metallurgy and Petroleum Engineers, p. 1211-1238.

Hickey, R.J., 1990, The geology of the Buckhorn mountain gold skarn, Okanagon County, Washington: unpublished M.S. thesis, Washington State University, 171 p.

Hietanen, A., 1962, Metasomatic metamorphism in western Clearwater County, Idaho: United States Geological Survey, Professional Paper 344-A, p. A1-A116.

Hodgson, C.J., 1975, The geology and geological development of the Broken Hill lode in the New Broken Hill Consolidated mine, Australia; Part II, Mineralogy: Geological Society of Australia, Journal, v. 22, p. 33-50.

Imai, H. and Yamazaki, S., 1967, Hydrothermal dolomite-rocks associated with hematite deposits of the Akatani mine, Niigata Prefecture, northeastern Japan: Waseda University School Science Engineering, Memoir 31, p. 11-63.

Ishihara, S., 1977, The magnetite-series and ilmenite-series granitic rocks: Mining Geology, v. 27, p. 293-305.

James, L.P., 1976, Zoned alteration in limestone at porphyry copper deposits, Ely, Nevada: Economic Geology, v. 71, p. 488-512.

Johnson, C.A., Rye, D.M. and Skinner, B.J., 1990, Petrology and stable isotope geochemistry of the metamorphosed zinc-iron-manganese deposit at Sterling Hill, New Jersey: Economic Geology, v. 85, p. 1133-1161.

Johnson, J.W. and Norton, D., 1985, Theoretical prediction of hydrothermal conditions and chemical equilibria during skarn formation in porphyry copper systems: Economic Geology, v. 80, p. 1791-1823.

Johnson, V.Y. and Keith, J.D., 1991, Petrology and geochemistry of the Springer scheelite skarn deposit, Mill City, Nevada, in Raines, G.L., Lisle, R.E., Schafer, R.W. and Wilkinson, W.H., eds., Geology and Ore Deposits of the Great Basin: Geological Society of Nevada, Reno, v. 1, p. 553-578.

Kato, Y., 1989, Rare earth elements in the skarn-type deposits in Japan: Mining Geology, v. 39, p. 62.

Kerrick, D.M., 1974, Review of Metamorphic Mixed Volatile (H_2O-CO_2) Equilibria: American Mineralogist, v. 59, p. 729-762.

Kesler, S.E., 1968, Contact-localized ore formation in the Memé mine, Haiti: Economic Geology, v. 63, p. 541-552.

Knopf, A., 1918, Geology and ore deposits of the Yerington District, NV: United States Geological Survey, Professional Paper 114, 68p.

Knopf, A., 1942, Ore deposition in the pyrometasomatic deposits, in Newhouse, W.H., ed., Ore Deposits as Related to Structural Features: Princeton University Press, p. 63-72.

Korzhinskii, D.S., 1948, Petrology of the Tur'insk skarn deposits of copper: Academy Nauk SSSR, Institute of Geology Nauk Trudy, vvp. 68, Ser. Rudnykh Mestorozhdenii, No. 10, 147 p.

Kulikov, I.V. and Boyarskaya, R.V., 1989, Hydrosaline melts in inclusions in fluorite from the Tyrnyauz Deposit: International Geology Review, v. 31, p. 1039-1054.

Kwak, T.A.P., 1978a, The conditions of formation of the King Island scheelite contact skarn, King Island, Tasmania, Australia: American Journal of Science, v. 278, p. 969-999.

Kwak, T.A.P., 1978b, Mass balance relationships and skarn forming processes at the King Island scheelite deposit, King Island, Tasmania, Australia: American Journal of Science, v. 278, p. 943-968.

Kwak, T.A.P., 1986, Fluid inclusions in skarns (carbonate replacement deposits): Journal of Metamorphic Geology, v. 4, p. 363-384.

Kwak, T.A.P., 1987, W-Sn skarn deposits and related metamorphic skarns and granitoids: Developments in Economic Geology, No. 24, Elsevier, Amsterdam, 451 p.

Kwak, T.A.P. and Abeysinghe, P.B., 1987, Rare earth and uranium minerals present as daughter crystals in fluid inclusions, Mary Kathleen U-REE skarn, Queensland, Australia: Mineralogical Magazine, v. 51, pt. 5, p. 665-670.

Kwak, T.A.P. and Askins, P.W., 1981, Geology and genesis of the F-Sn-W-(Be-Zn) skarn (wrigglite) at Moina, Tasmania: Economic Geology, v. 76, p. 439-467.

Kwak, T.A.P. and Tan, T.H., 1981, The geochemistry of zoning in skarn minerals at the King Island (Dolphin) mine: Economic Geology, v. 76, p. 468-497.

Kwak, T.A.P. and White, A.J.R., 1982, Contrasting W-Mo-Cu and W-Sn-F skarn types and related granitoids: Mining Geology, v. 32, p. 339-351.

Kyle, J.R., Rubin, J.N., McMahon, T.P. and McDowell, F., 1991, Preliminary investigations of porphyry-skarn copper-gold orebodies, Ertsberg (Gunung Bijih) district, Irian Jaya, Indonesia: Geological Association of Canada-Mineralogical Association of Canada-Society of Economic Geologists, Program with Abstracts, v. 16, p. A69.

Lamey, C.A., 1948, Contact Metasomatic iron deposits of California: Geological Society of America, Bulletin, v. 72, p. 669-678.

Lamey, C.A., 1961, Contact metasomatic iron deposits of California: Geological Society of America, Bulletin, v. 72, p. 669-678.

Layne, G.D. and Spooner, E.T.C., 1991, The JC tin skarn deposit, southern Yukon Territory: I. Geology, paragenesis, and fluid inclusion microthermometry: Economic Geology, v. 86, p. 29-47.

Layne, G.D., Longstaffe, F.J. and Spooner, E.T.C., 1991, The JC tin skarn deposit, southern Yukon Territory: II. A carbon, oxygen, hydrogen, and sulfur stable isotope study: Economic Geology, v. 86, p. 48-65.

Lentz, D., 1991, Radioelement distribution in U, Th, Mo, and rare-earth-element pegmatites, skarns, and veins in a portion of the Grenville Province, Ontario and Quebec: Canadian Journal of Earth Sciences, v. 28, p. 1-12.

Lhotka, P.G., 1988, Geology and geochemistry of gold-bearing iron formation in the Contwoyto Lake-Point Lake region, Northwest Territories, Canada: unpublished Ph.D. thesis, University of Alberta, Edmonton, 265 p.

Lhotka, P.G. and Nesbitt, B.E., 1989, Geology of unmineralized and gold-bearing iron formation, Contwoyto Lake-Point Lake region, Northwest Territories, Canada: Canadian Journal of Earth Sciences, v. 26, p. 46-64.

Lindgren, W., 1902, The character and genesis of certain contact deposits: American Institute of Mining Engineers, Transactions, v. 31, p. 226-244.

Lyons, J.I., 1988, Volcanogenic iron oxide deposits, Cerro de Mercado and vicinity, Durango, Mexico: Economic Geology, v. 83, p. 1886-1906.

Marcke de Lummen, G. van, 1988, Oxygen and hydrogen isotope evidence for influx of magmatic water in the formation of W-Mo- and Sn-bearing skarns in pelitic rocks at Costaboone, France, and Land's End, England, in Zachrisson, E., ed., Proceedings of the 7th Quadrennial IAGOD Symposium: E. Schweizerbart'sche Verlagsbuchhandlung, Stuttgart, p. 355-362.

Mathieson, G.A. and Clark, A.H., 1984, The Can-Tung E zone scheelite skarn ore body, Tungsten, Northwest Territories: a revised genetic model: Economic Geology, v. 79, p. 883-901.

McDowell, S.D. and Elders, W.A., 1980, Authigenic layer silicate minerals in Borehole Elmore 1, Salton Sea geothermal field, California, USA.: Contributions to Mineralogy and Petrology, v. 74, p. 293-310.

Megaw, P.K.M., Ruiz, J. and Titley, S.R., 1988, High-temperature, carbonate-hosted Ag-Pb-Zn(Cu) deposits of northern Mexico: Economic Geology, v. 83, p. 1856-1885.

Meinert, L.D., 1983, Variability of skarn deposits — Guides to exploration, in Boardman, S.J., ed., Revolution in the Earth Sciences: Kendall-Hunt Publishing Co., p. 301-316.

Meinert, L.D., 1984, Mineralogy and petrology of iron skarns in western British Columbia, Canada: Economic Geology, v. 79, p. 869-882.

Meinert, L.D., 1987, Skarn zonation and fluid evolution in the Groundhog Mine, Central Mining District, New Mexico: Economic Geology, v. 82, p. 523-545.

Meinert, L.D., 1989, Gold skarn deposits — Geology and exploration criteria, in Groves, D., Keays, R. and Ramsay, R., eds., Proceedings of Gold '88: Economic Geology, Monograph 6, p. 537-552.

Meinert, L.D., Brooks, J.W. and Myers, G.L., 1990, Whole rock geochemistry and contrast among skarn types, in Meinert, L.D., ed., Skarn deposits in Nevada, Great Basin Symposium — Geology and ore deposits of the Great Basin: Geological Society of Nevada, Fieldtrip 2 Guidebook, p. 179-192.

Mueller, A.G., 1988, Archaean Gold-Silver Deposits with Prominent Calc-Silicate Alteration in the Southern Cross Greenstone Belt, Western Australia: Analogues of Phanerozoic Skarn Deposits, in Ho, S.E, and Groves, D.I., eds., Advances in Understanding Precambrian Gold Deposits, Vol. 2: Geology Department and University Extension, University of Western Australia, Publication 12, p. 141-163.

Myers, G.L. and Meinert, L.D., 1991, Alteration, mineralization, and gold distribution in the Fortitude gold skarn, in Raines, G.L., Lisle, R.E., Schafer, R.W. and Wilkinson, W.H., eds., Geology and Ore Deposits of the Great Basin: Geological Society of Nevada, Reno, v. 1, p. 407-418.

Nakano, T., Shimazaki, H. and Shimizu, M., 1990, Strontium isotope systematics and metallogenesis of skarn deposits in Japan: Economic Geology, v. 85, p. 794-815.

Newberry, R., 1987, Use of intrusive and calc-silicate compositional data to distinguish contrasting skarn types in the Darwin polymetallic skarn district, California, USA: Mineralium Deposita, v. 22, p. 207-215.

Newberry, R., 1991, Scheelite-bearing skarns in the Sierra Nevada Region, California: Contrasts in zoning and mineral compositions and tests of infiltration metasomatism theory, in Skarns — Their Genesis and Metallogeny: Theophrastus Publications S.A., Athens, p. 343-384.

Newberry, R.J., 1982, Tungsten-bearing skarns of the Sierra Nevada. I. The Pine Creek Mine, California: Economic Geology, v. 77, p. 823-844.

Newberry, R.J., 1983, The formation of subcalcic garnet in scheelite-bearing skarns: Canadian Mineralogist, v. 21, p. 529-544.

Newberry, R.J. and Einaudi, M.T., 1981, Tectonic and geochemical setting of tungsten skarn mineralization in the Cordillera: Arizona Geological Society, Digest, v. 14, p. 99-112.

Newberry, R.J. and Swanson, S.E., 1986, Scheelite skarn granitoids: An evaluation of the roles of magmatic source and process: Ore Geology Reviews, v. 1, p. 57-81.

Newberry R.J., Burns, L.E., Swanson, S.E. and Smith, T.E., 1990, Comparative petrologic evolution of the Sn and W granites of the Fairbanks-Circle area, interior Alaska, in Stein, H.J. and Hannah, J.L., eds, Ore-bearing granite systems; Petrogenesis and mineralizing processes: Geological Society of America, Special Paper 246, p. 121-142.

Nielson, R.L., 1970, Mineralization and alteration in calcareous rocks near the Santa Rita stock, New Mexico: New Mexico Geological Society, Guidebook, 21st Field Conference, p. 133-139.

Norton, D., 1982, Fluid and heat transport phenomena typical of copper-bearing pluton environments, southeastern Arizona: in Titley, S.R., ed., Advances in Geology of Porphyry Copper Deposits: Southwestern North America: University of Arizona Press, Tucson, p. 59-72.

Pan, Y., Fleet, M.E. and Stone, W.E., 1991, Skarn mineralization (Cr, Fe, Au) in an Archean greenstone belt, White River Property, Hemlo area, Ontario: Economic Geology, v. 86, p. 1626-1645.

Permingeat, F., 1957, Le gisement de molybdène, tungstène et cuivre d'Azègour (Haut Atlas), étude pétrographique et metallogénique: Maroc Service Geological Notes et Memoir 141, 284 p.

Phan, K.D., 1969, Skarns et minéralisations associés: Chronique Mines Recherches Minière, v. 37, p. 292-311, 339-362.

Purtov, V.K., Kholodnov, V.V., Anfilogov, V.N. and Nechkin, G.S., 1989, The role of chlorine in the formation of magnetite skarns: International Geology Reviews, v. 31, p. 63-71.

Ray, G.E., Dawson, G.L. and Simpson, R., 1988, Geology, geochemistry and metallogenic zoning in the Hedley Gold-Skarn Camp: British Columbia Ministry of Energy, Mines and Petroleum Resources, Geological Fieldwork, 1987, Paper 1988-1, p. 59-80.

Ray, G.E. and Webster, I.C.L., 1991a, An overview of skarn deposits, in Ore deposits, tectonics and metallogeny in the Canadian cordillera: British Columbia Ministry of Energy, Mines and Petroleum Resources, Paper 1991-4, p. 213-252.

Ray, G.E. and Webster, I.C.L., 1991b, Geology and mineral occurrences of the Merry Widow skarn camp: British Columbia Ministry of Energy, Mines and Petroleum Resources, Open File Map 1991-8.

Ripley, E.M. and Ohmoto, H., 1977, Mineralogic, sulfur isotope, and fluid inclusion studies of the stratabound copper deposits at the Raul mine, Peru: Economic Geology, v. 72, p. 1017-1041.

Roedder, E., 1984, Fluid Inclusions: Mineralogical Society of America, Reviews in Mineralogy, v. 12, 644 p.

Salemink, J. and Schuiling, R.D., 1987, A two-stage, transient heat and mass transfer model for the granodiorite intrusion at Seriphos, Greece, and the associated formation of contact metasomatic skarn and Fe-ore deposits, in Helgeson, H.C., ed., Chemical transport in metasomatic processes: Department Geology and Geophysics, University of California, Berkeley, NATO Advanced Study Institutes Series C; Mathematical and Physical Sciences 218, p. 547-575.

Sangster, D.F., 1969, The contact metasomatic magnetite deposits of southwestern British Columbia: Geological Survey of Canada, Bulletin 172, 79 p.

Sawkins, F.J., 1984, Metal deposits in relation to plate tectonics: Minerals and Rocks Series, no. 17, Springer-Verlag, Berlin, 325 p.

Schmidt, E.A. and Worthington, J., 1977, Geology and mineralization of the Cannivan Gulch molybdenum deposit, Beaverhead County, Montana: Geological Association of Canada-Mineralogical Association of Canada, Program with Abstracts, v. 2, p. 46.

Shelton, K.L., 1983, Composition and origin of ore-forming fluids in a carbonate-hosted porphyry copper and skarn deposit: A fluid inclusion and stable isotope study of Mines Gaspé, Quebec: Economic Geology, v. 78, p. 387-421.

Shelton, K.L. and Rye, D.M., 1982, Sulfur isotopic composition of ores from Mines Gaspé, Quebec: An example of sulfate-sulfide isotopic disequilibria in ore-forming fluids with applications to other porphyry-type deposits: Economic Geology, v. 77, p. 1688-1709.

Sheppard, S.M.F., Nielson, R.L. and Taylor, H.P., Jr., 1971, Hydrogen and oxygen isotope ratios in minerals from porphyry copper deposits: Economic Geology, v. 66, p. 515-542.

Shimazaki, H., 1980, Characteristics of skarn deposits and related acid magmatism in Japan: Economic Geology, v. 75, p. 173-183.

Shimazaki, H., 1988, Oxygen, carbon, and sulfur isotope study of skarn deposits in Japan, in Zachrisson, E., ed., Proceedings of the 7th Quadrennial IAGOD Symposium: E. Schweizerbart'sche Verlagsbuchhandlung, Stuttgart, p. 375-381.

Shimizu, M. and Iiyama, J.T., 1982, Zinc-lead skarn deposits of the Nakatatsu mine, Central Japan: Economic Geology, v. 77, p. 1000-1013.

Sidder, G.B., 1984, Ore genesis at the Monterrosas Deposit in the Coastal Batholith, Ica, Peru: unpublished Ph.D. thesis, Oregon State University, 247 p.

Silva, K.K.M.W. and Siriwardena, C.H.E.R., 1988, Geology and the origin of the corundum-bearing skarn at Bakamuna, Sri Lanka: Mineralium Deposita, v. 23, p. 186-190.

Smirnov, V.I., 1976, Skarn deposits, in Geology of Mineral Deposits: MIR Publ., Moscow, p. 156-188.

Sokolov, G.A. and Grigorev, V.M., 1977, Deposits of iron, in Smirnov, V.I., ed., Ore deposits of the USSR: Pittman, London, v. 1, p. 7-113.

Soler, A., Ayora, C., Cardellach, E. and Delgado, J., 1990, Gold-bearing hedenbergite skarns from the SW contact of the Andorra granite (Central Pyrenees, Spain): Mineralium Deposita, v. 25 (Supplement), p. S59-S68.

Spector, A., 1972, Examples of the use of aeromagnetic surveying in the search for porphyry and skarn copper deposits: Society of Exploration Geophysicists, Annual International Meeting, No. 42, p. 7-8.

Takahashi, M., Aramake, S. and Ishihara, S., 1980, Magnetite-series/ilmenite-series vs. I-type/S-type granitoids: Japanese Society of Mining and Geology, v. 8, p. 13-28.

Tan, T.H. and Kwak, T.A.P., 1979, The measurement of the thermal history around the Grassy Granodiorite, King Island, Tasmania, by use of fluid inclusion data: Journal of Geology, v. 87, p. 43-54.

Taylor, B.E., 1976, Origin and significance of C-O-H fluids in the formation of Ca-Fe-Si skarn, Osgood Mountains, Humboldt County, Nevada: unpublished Ph.D. thesis, Stanford University, 149 p.

Taylor, B.E. and O'Neil, J.R., 1977, Stable isotope studies of metasomatic Ca-Fe-Al-Si skarns and associated metamorphic and igneous rocks, Osgood Mountains, Nevada: Contributions to Mineralogy and Petrology, v. 63, pp 1-49.

Theodore, T.G. and Blake, D.W., 1975, Geology and geochemistry of the Copper Canyon porphyry copper deposit and surrounding area, Lander County, Nevada: United States Geological Survey, Professional Paper 798-B, 86 p.

Theodore, T.G. and Blake, D.W., 1978, Geology and geochemistry of the West orebody and associated skarns, Copper Canyon porphyry copper deposits, Lander County, Nevada (with a section on electron microprobe analyses of andradite and diopside by N.G. Banks): United States Geological Survey, Professional Paper 798-C, 85 p.

Theodore, T.G., Orris, G.J., Hammarstrom, J.M. and Bliss, J.D., 1991, Gold-bearing skarns: United States Geological Survey, Bulletin 1930, 61 p.

Umpleby, J.B., 1913, Geology and ore deposits of Lemhi County, Idaho: United States Geological Survey, Bulletin 528, 182 p.

Vidal, C., Injoque-Espinoza, J., Sidder, G.B. and Mukasa, S.B., 1990, Amphibolitic Cu-Fe skarn deposits in the central coast of Peru: Economic Geology, v. 85, p. 1447-1461.

Vidale, R., 1969, Metasomatism in a chemical gradient and the formation of calc-silicate bands: American Journal of Science, v. 267, p. 857-874.

Vokes, F., 1963, Molybdenum deposits of Canada: Geological Survey of Canada, Economic Geology Report 20, 332 p.

Wallmach, T. and Hatton, C.J., 1989, Extreme facies of contact metamorphism developed in calc-silicate xenoliths in the eastern Bushveld complex: The Canadian Mineralogist, v. 27, p. 509-523.

Watanabe, T., 1960, Characteristic features of ore deposits found in contact metamorphic aureoles in Japan: International Geology Review, v. 2, p. 946-966.

Wesoloski, D., 1984, Geochemistry of tungsten in scheelite deposits: The skarn ores at King Island, Tasmania: unpublished Ph.D. thesis, Pennsylvania State University, 430 p.

Wilson, M., 1989, Igneous Petrogenesis; A Global Tectonic Approach: Unwin Hyman, London, 466 p.

Wood, S.A., Mountain, B.W. and Fenlon, B.J., 1989, Thermodynamic constraints on the solubility of platinum and palladium in hydrothermal solutions; reassessment of hydroxide, bisulfide, and ammonia complexing: Economic Geology, v. 84, p. 2020-2028.

Wotruba, P.R., Benson, R.G. and Schmidt, K.W., 1988, Geology of the Fortitude gold-silver skarn deposit, Copper Canyon, Lander County, Nevada, in Schafer, R.W., Cooper, J.J. and Vikre, P.G., eds., Bulk mineable precious metal deposits of the western United States: Geological Society of Nevada, Reno, p. 159-172.

Yu, Huilung, 1985, Skarns in the Xujiachong picrite body, Jingshan County, Hubei: Acta Petrologica, Mineralogica et Analytica, v. 4, pt. 2, p. 108-113.

Zarayskiy, G.P., Zharikov, V.A., Stoyanovskaya, F.M. and Balashov, V.N., 1987, The experimental study of bimetasomatic skarn formation: International Geology Review, v. 29, p. 761-858.

Zharikov, V.A., 1970, Skarns: International Geology Review, v. 12, p. 541-559, 619-647, 760-775.

Zierenberg, R.A. and Shanks, W.C., III, 1983, Mineralogy and geochemistry of epigenetic features in metalliferous sediment, Atlantis II Deep, Red Sea: Economic Geology, v. 78, p. 57-72.